compared the kinetics of CFSE$^+$Vβ4$^+$ (AN3$^+$) and CFSE$^+$Vβ4$^-$ (AN3$^-$) CD4$^+$ T cells. The percentage of Vβ4$^+$ cells in CFSE$^+$ CD4$^+$ T cells in red pulp was significantly higher than that in white pulp 3 and 5 h after the transfer (Fig. 6*A*). The difference disappeared 18 h after the transfer. Though basal CD69 expression was comparable between CFSE$^+$Vβ4$^+$ CD4$^+$ cells and CFSE$^+$ Vβ4$^-$ CD4$^+$ T cells, CD69 expression of CFSE$^+$Vβ4$^+$ CD4$^+$ cells was significantly increased compared with that of CFSE$^+$Vβ4$^-$ CD4$^+$ T cells 8 h after the transfer (Fig. 6*B*). These results indicated that nucleosome-specific T cells were initially retained in the red pulp and activated during this retention phase.

Discussion

In this study, we observed potent nucleosome autoantigen stimulation of T cells by splenic phagocytes, including F4/80$^+$ macrophages. Reconstitution of nucleosome-specific T cells enabled better understanding of autoantigen presentation in lupus-prone mice. Because F4/80$^+$ macrophages from the thymus and BM presented nucleosomes very weakly, apoptosis in lymphoid organs may not simply explain nucleosome presentation. Splenic macrophages play a significant role in trapping particulate Ags in circulation (31, 32). This is the reason for the severe depletion of splenic macrophages by Cl_2MDP-liposome treatment. Nucleosomes are abundant particulate autoantigens generated by cellular apoptosis. Because serum nucleosome levels have been reported to be elevated in SLE patients (33), it suggests that nucleosomes are generated in various organs and enter the circulation. Therefore, we speculate that splenic phagocytes including F4/80$^+$ macrophages take up apoptotic debris and present nucleosomes specifically to T cells.

The increased expression of MHC class II in NZB/W F4/80$^+$ macrophages may be associated with pathogenic autoantigen presentation of this APC population. Because NZB/W and parental NZB F4/80$^+$ macrophages exhibited similar MHC class II expression levels (Fig. 1*D*), the increased expression of MHC class II in NZB/W F4/80$^+$ macrophages is probably influenced by genetic background. The increased expression of MHC class II in NZB F4/80$^+$ macrophages may be associated with autoimmune hemolytic anemia in NZB mice. In contrast, unknown apoptotic mechanisms specific to the spleen may be associated with splenic nucleosome presentation.

Our data also reveals an apparent paradoxical role of phagocytes in lupus. As shown in MFG-E8$^{-/-}$ mice (6) and *Mer*^{kd} mice (7), impaired clearance of apoptotic cells by macrophages predisposes to lupus-like disease. In contrast, macrophages themselves are responsible for autoantigen presentation, which drives autoimmunity. In addition to our study, macrophages promote development and activation of β cell-specific T cells in NOD mice (34). The balance between clearance of apoptotic cells and autoantigen presentation seems important, because 10–15 injections of Cl_2MDP-liposomes exacerbated lupus disease (35). Moreover, reduction of autoantibody titer may not fully ameliorate advanced stage of the disease. Clodronate-liposome insensitive population (e.g., cytotoxic CD8 T cells and neutrophils) may contribute to the late phase of disease progression. In our experiment, a few injections of Cl_2MDP-liposomes delayed the development of lupus. Transient depletion of splenic phagocytes was effective in suppressing autoantigen presentation, autoantibody production, and disease progression.

Depletion of splenic phagocytes was associated with the reduction of autoantigen-specific PCs. In Fig. 3*B*, production of anti-nucleosome Ab was severely impaired after depletion of splenic phagocytes. This profound suppression of anti-nucleosome Ab is consistent with the decrease of nuc-specific PCs both in the spleen and in the BM described in Fig. 4*B*. In contrast, the suppression of anti-dsDNA titer was only around 50% after depletion of splenic phagocytes. We suppose that this partial suppression of anti-dsDNA Ab is associated with the survival of dsDNA-specific PCs in the BM. The spleens of NZB/W F$_1$ mice contain ~10 times more PCs than those of normal mice, though PCs are not significantly increased in the BM (22). Less than 60% of the splenic Ab-secreting cells are short-lived PCs. These splenic short-lived PCs are sensitive to cyclophosphamide (short-lived PCs are eliminated 1 wk after cyclophosphamide treatment). Investigators have shown that survival of long-lived PCs is dependent on a supportive environment, i.e., specific survival niches which can be found in the BM, inflamed tissue, and the normal spleen (36). Whether splenic phagocyte depletion by Cl_2MDP-liposomes affects survival niches for PCs directly or indirectly should be addressed further.

F4/80$^+$ macrophages are located in the splenic red pulp where plasmablasts and PCs migrate after Ag-specific differentiation (32, 37). We showed activation-associated retention of nucleosome-specific T cells in red pulp. Because nucleosome-specific T cells appeared to migrate to white pulp 18 h after the transfer, initial activation of T cells in red pulp may be an important stimulation for autoantigen priming.

In summary, splenic phagocytes present autoantigen significantly and support autoantibody production in lupus-prone mice. Suppressing autoantigen presentation by splenic phagocytes without affecting the clearance of apoptotic bodies would be a novel therapeutic approach for systemic autoimmune disease.

Acknowledgments

We are grateful to Yayoi Tsukahara and Kayako Watada for excellent technical assistance.

Disclosures

The authors have no financial conflict of interest.

References

1. Vratsanos, G. S., S. Jung, Y. M. Park, and J. Craft. 2001. CD4$^+$ T cells from lupus-prone mice are hyperresponsive to T cell receptor engagement with low and high affinity peptide antigens: a model to explain spontaneous T cell activation in lupus. *J. Exp. Med.* 193: 329–337.
2. Desai-Mehta, A., L. Lu, R. Ramsey-Goldman, and S. K. Datta. 1996. Hyperexpression of CD40 ligand by B and T cells in human lupus and its role in pathogenic autoantibody production. *J. Clin. Invest.* 97: 2063–2073.
3. Ishikawa, S., T. Sato, M. Abe, S. Nagai, N. Onai, H. Yoneyama, Y. Zhang, T. Suzuki, S. Hashimoto, T. Shirai, et al. 2001. Aberrant high expression of B lymphocyte chemokine (BLC/CXCL13) by C11b$^+$CD11c$^+$ dendritic cells in murine lupus and preferential chemotaxis of B1 cells towards BLC. *J. Exp. Med.* 193: 1393–1402.
4. Wofsy, D., C. E. Kerger, and W. E. Seaman. 1984. Monocytosis in the BXSB model for systemic lupus erythematosus. *J. Exp. Med.* 159: 629–634.
5. Muller, M., A. Emmendorffer, and M. L. Lohmann-Matthes. 1991. Expansion and high proliferative potential of the macrophage system throughout life time of lupus-prone NZB/W and MRL lpr/lpr mice: lack of down-regulation of extramedullar macrophage proliferation in the postnatal period. *Eur. J. Immunol.* 21: 2211–2217.
6. Hanayama, R., M. Tanaka, K. Miyasaka, K. Aozasa, M. Koike, Y. Uchiyama, and S. Nagata. 2004. Autoimmune disease and impaired uptake of apoptotic cells in MFG-E8-deficient mice. *Science* 304: 1147–1150.
7. Scott, R. S., E. J. McMahon, S. M. Pop, E. A. Reap, R. Caricchio, P. L. Cohen, H. S. Earp, and G. K. Matsushima. 2001. Phagocytosis and clearance of apoptotic cells is mediated by MER. *Nature* 411: 207–211.
8. Steinman, R. M., D. Hawiger, and M. C. Nussenzweig. 2003. Tolerogenic dendritic cells. *Annu. Rev. Immunol.* 21: 685–711.
9. Fadok, V. A., D. L. Bratton, A. Konowal, P. W. Freed, J. Y. Westcott, and P. M. Henson. 1998. Macrophages that have ingested apoptotic cells in vitro inhibit proinflammatory cytokine production through autocrine/paracrine mechanisms involving TGF-β, PGE2, and PAF. *J. Clin. Invest.* 101: 890–898.
10. McDonald, P. P., V. A. Fadok, D. Bratton, and P. M. Henson. 1999. Transcriptional and translational regulation of inflammatory mediator production by endogenous TGF-β in macrophages that have ingested apoptotic cells. *J. Immunol.* 163: 6164–6172.
11. Vall, R. E., M. Herrmann, E. A. Roth, C. Stach, J. R. Kalden, and I. Girkontaite. 1997. Immunosuppressive effects of apoptotic cells. *Nature* 390: 350–351.
12. Heil, F., H. Hemmi, H. Hochrein, F. Ampenberger, C. Kirschning, S. Akira, G. Lipford, H. Wagner, and S. Bauer. 2004. Species-specific recognition of single-stranded RNA via toll-like receptor 7 and 8. *Science* 303: 1526–1529.

13. Mohan, C., S. Adams, V. Stanik, and S. K. Datta. 1993. Nucleosome: a major immunogen for pathogenic autoantibody-inducing T cells of lupus. *J. Exp. Med.* 177: 1367–1381.
14. Kaliyaperumal, A., C. Mohan, W. Wu, and S. K. Datta. 1996. Nucleosomal peptide epitopes for nephritis-inducing T helper cells of murine lupus. *J. Exp. Med.* 183: 2459–2469.
15. Caseiola-Rosen, L. A., G. Anhalt, and A. Rosen. 1994. Autoantigens targeted in systemic lupus erythematosus are clustered in two populations of surface structures on apoptotic keratinocytes. *J. Exp. Med.* 179: 1317–1330.
16. Radic, M., T. Marion, and M. Monestier. 2004. Nucleosomes are exposed at the cell surface in apoptosis. *J. Immunol.* 172: 6692–6700.
17. Bruns, A., S. Blass, G. Hausdorf, G. R. Burmester, and F. Hiepe. 2000. Nucleosomes are major T and B cell autoantigens in systemic lupus erythematosus. *Arthritis Rheum.* 43: 2307–2315.
18. Amoura, Z., H. Chabre, S. Koutouzov, C. Lotton, A. Cabrespines, J. F. Bach, and L. Jacob. 1994. Nucleosome-restricted antibodies are detected before anti-dsDNA and/or antihistone antibodies in serum of MRL-Mp lpr/lpr and +/+ mice, and are present in kidney eluates of lupus mice with proteinuria. *Arthritis Rheum.* 37: 1684–1688.
19. Fujio, K., A. Okamoto, H. Tahara, M. Abe, Y. Jiang, T. Kitamura, S. Hirose, and K. Yamamoto. 2004. Nucleosome-specific regulatory T cells engineered by triple gene transfer suppress a systemic autoimmune disease. *J. Immunol.* 173: 2118–2125.
20. Fujio, K., Y. Misaki, K. Setoguchi, S. Morita, K. Kawahata, I. Kato, T. Nosaka, K. Yamamoto, and T. Kitamura. 2000. Functional reconstitution of class II MHC-restricted T cell immunity mediated by retroviral transfer of the $\alpha\beta$ TCR complex. *J. Immunol.* 165: 528–532.
21. Morita, S., T. Kojima, and T. Kitamura. 2000. Plat-E: an efficient and stable system for transient packaging of retroviruses. *Gene Ther.* 7: 1063–1066.
22. Hoyer, B. F., K. Moser, A. E. Hauser, A. Peddinghaus, C. Voigt, D. Eilat, A. Radbruch, F. Hiepe, and R. A. Manz. 2004. Short-lived plasmablasts and long-lived plasma cells contribute to chronic humoral autoimmunity in NZB/W mice. *J. Exp. Med.* 199: 1577–1584.
23. Van Rooijen, N., and A. Sanders. 1994. Liposome mediated depletion of macrophages: mechanism of action, preparation of liposomes and applications. *J. Immunol. Methods* 174: 83–93.
24. Takahashi, S., M. Nose, J. Sasaki, T. Yamamoto, and M. Kyogoku. 1991. IgG3 production in MRL/lpr mice is responsible for development of lupus nephritis. *J. Immunol.* 147: 515–519.
25. Inoue, A., H. Hasegawa, M. Kohno, M. R. Ito, M. Terada, T. Imai, O. Yoshie, M. Nose, and S. Fujita. 2005. Antagonist of fractalkine (CX3CL1) delays the initiation and ameliorates the progression of lupus nephritis in MRL/lpr mice. *Arthritis Rheum.* 52: 1522–1533.
26. Muraoka, M., H. Hasegawa, M. Kohno, A. Inoue, T. Miyazaki, M. Terada, M. Nose, and M. Yasukawa. 2006. IK cytokine ameliorates the progression of lupus nephritis in MRL/lpr mice. *Arthritis Rheum.* 54: 3591–3600.
27. Cassese, G., S. Lindenau, B. de Boer, S. Arce, A. Hauser, G. Riemekasten, C. Berek, F. Hiepe, V. Krenn, A. Radbruch, and R. A. Manz. 2001. Inflamed kidneys of NZB/W mice are a major site for the homeostasis of plasma cells. *Eur. J. Immunol.* 31: 2726–2732.
28. Zhang, D., K. Fujio, Y. Jiang, J. Zhao, N. Tada, K. Sudo, H. Tsurui, K. Nakamura, K. Yamamoto, H. Nishimura, et al. 2004. Dissection of the role of MHC class II A and E genes in autoimmune susceptibility in murine lupus models with intragenic recombination. *Proc. Natl. Acad. Sci. USA* 101: 13838–13843.
29. Michaels, M. A., H. K. Kang, A. Kaliyaperumal, E. Satyaraj, Y. Shi, and S. K. Datta. 2005. A defect in deletion of nucleosome-specific autoimmune T cells in lupus-prone thymus: role of thymic dendritic cells. *J. Immunol.* 175: 5857–5865.
30. Lo, C. G., T. T. Lu, and J. G. Cyster. 2003. Integrin-dependence of lymphocyte entry into the splenic white pulp. *J. Exp. Med.* 197: 353–361.
31. Aichele, P., J. Zinke, L. Grode, R. A. Schwendener, S. H. Kaufmann, and P. Seiler. 2003. Macrophages of the splenic marginal zone are essential for trapping of blood-borne particulate antigen but dispensable for induction of specific T cell responses. *J. Immunol.* 171: 1148–1155.
32. Mebius, R. E., and G. Kraal. 2005. Structure and function of the spleen. *Nat. Rev. Immunol.* 5: 606–616.
33. Amoura, Z., J. C. Piette, H. Chabre, P. Cacoub, T. Papo, B. Wechsler, J. F. Bach, and S. Koutouzov. 1997. Circulating plasma levels of nucleosomes in patients with systemic lupus erythematosus: correlation with serum antinucleosome antibody titers and absence of clear association with disease activity. *Arthritis Rheum.* 40: 2217–2225.
34. Jun, H. S., C. S. Yoon, L. Zbytnuik, N. van Rooijen, and J. W. Yoon. 1999. The role of macrophages in T cell-mediated autoimmune diabetes in nonobese diabetic mice. *J. Exp. Med.* 189: 347–358.
35. Denny, M. F., P. Chandaroy, P. D. Killen, R. Carecchio, E. E. Lewis, B. C. Richardson, K. D. Lee, J. Gavalchin, and M. J. Kaplan. 2006. Accelerated macrophage apoptosis induces autoantibody formation and organ damage in systemic lupus erythematosus. *J. Immunol.* 176: 2095–2104.
36. Manz, R. A., S. Arce, G. Cassese, A. E. Hauser, F. Hiepe, and A. Radbruch. 2002. Humoral immunity and long-lived plasma cells. *Curr. Opin. Immunol.* 14: 517–521.
37. Sze, D. M., K. M. Toellner, C. Garcia de Vinuesa, D. R. Taylor, and I. C. MacLennan. 2000. Intrinsic constraint on plasmablast growth and extrinsic limits of plasma cell survival. *J. Exp. Med.* 192: 813–821.

Aberrant Genetic Control of Invariant TCR-Bearing NKT Cell Function in New Zealand Mouse Strains: Possible Involvement in Systemic Lupus Erythematosus Pathogenesis[1]

Kazuyuki Tsukamoto,* Mareki Ohtsuji,* Wakana Shiroiwa,*† Qingshun Lin,*† Kazuhiro Nakamura,* Hiromichi Tsurui,* Yi Jiang,¶ Katsuko Sudo,‡ Hiroyuki Nishimura,§ Toshikazu Shirai,* and Sachiko Hirose[2]*

Both suppressive and promoting roles of NKT cells have been reported in the pathogenesis of systemic lupus erythematosus (SLE). Herein, we found that although New Zealand mice have normal frequencies of NKT cells, their in vitro potential to produce IL-4 and IFN-γ in response to α-galactosylceramide was remarkably impaired in New Zealand Black (NZB) mice prone to mild SLE, while production was highly up-regulated in nonautoimmune New Zealand White (NZW) mice and at intermediate levels in (NZB × NZW)F_1 mice, which are prone to severe SLE. Because this aberration is evident in young mice before disease onset, genetic mechanisms are thought to be involved. Genome-wide quantitative trait locus analysis and association studies revealed that a locus linked to *D11Mit14* on chromosome 11 may be involved in the difference in cytokine-producing potential between NZB and NZW NKT cells. Additionally, (NZB × NZW)F_1 × NZB backcross progeny with the NZW genotype for *D11Mit14* showed significantly increased frequencies of age-associated SLE phenotypes, such as high serum levels of IgG, IgG anti-DNA Abs, and lupus nephritis. In coculture studies, α-galactosylceramide-stimulated NKT cells from NZW and (NZB × NZW)F_1 mice, but not from NZB mice, showed significantly enhanced Ig synthesis by B cells. These findings suggest that the *D11Mit14*-linked NZW locus may contribute to the development of SLE in (NZB × NZW)F_1 mice through a mechanism that up-regulates NKT cell function. Thus, this NZW allele may be a candidate of the NZW modifiers that act to promote (NZB × NZW)F_1 disease. *The Journal of Immunology*, 2008, 180: 4530–4539.

Natural killer T cells belong to a lymphocyte lineage distinct from conventional T cells and bear both the NK cell marker NK1.1 and the conventional T cell marker CD3. Most human and mouse NKT cells express invariant TCR α-chain (Vα24Jα15 in humans and Vα14Jα281 in mice) (1–5) and are strongly activated in vivo and in vitro by glycolipid Ags such as α-galactosylceramide (α-GalCer)[3] (3) presented by CD1d, a nonclassical MHC class I-like Ag-presenting molecule expressed on the surface of APCs (6, 7). When activated, NKT cells rapidly produce large amounts of various cytokines and trigger the activation of a variety of immune cells (1–5).

Accumulated evidence has shown that the number and function of NKT cells are reduced in patients with various autoimmune diseases, including type I diabetes (8, 9), systemic sclerosis (10–12), rheumatoid arthritis (11, 12), multiple sclerosis (13, 14), and systemic lupus erythematosus (SLE) (11, 12), suggesting that NKT cells play a suppressive role in autoimmune diseases. There are also publications that favor this hypothesis, reporting that type I diabetes-prone NOD mice have an intrinsic defect in the number and function of NKT cells, and that this defect is associated with disease development (15–17). Thus, the activation of NKT cells by repeated injections of α-GalCer or the introduction of transgenic Vα14 prevents spontaneous diabetes in NOD mice (18–20). Conversely, the absence of NKT cells in CD1d-deficient NOD mice increases the incidence of diabetes (21, 22). In MRL/*lpr* mice, invariant NKT cells are specifically reduced with aging (23), and repeated injections of α-GalCer prevent inflammatory dermatitis in these mice (24).

Activation of NKT cells by α-GalCer, or its derivative OCH, also protects against experimental autoimmune encephalomyelitis (25, 26) and collagen-induced arthritis (CIA) (27). However, the disease protection conferred by these glycolipids is not simply due to the increase in the number of NKT cells, but it correlates with their ability to suppress Th1 cell responses and/or to promote Th2 cell responses (25–27). Importantly, there are reports indicating that the incidence and the severity of CIA were reduced in NKT cell-deficient mice, as compared with findings in wild-type mice (27, 28). These observations are in contrast to those found in NKT cell-deficient NOD mice (23, 24). Thus, it was suggested that NKT cells function as not only suppressor but also effector cells in different types of autoimmune diseases.

*Department of Pathology and †Department of Obstetrics and Gynecology, Juntendo University School of Medicine; ‡Animal Research Center, Tokyo Medical University, Tokyo; §Toin Human Science and Technology Center, Department of Biomedical Engineering, Toin University of Yokohama, Yokohama, Japan; and ¶Central Laboratory of First Clinical College, China Medical University, Shenyang, China

Received for publication October 24, 2007. Accepted for publication January 30, 2008.

The costs of publication of this article were defrayed in part by the payment of page charges. This article must therefore be hereby marked *advertisement* in accordance with 18 U.S.C. Section 1734 solely to indicate this fact.

[1] This work was supported in part by Grants-in-Aid for Scientific Research on Priority Areas and for Center of Excellence Research from the Ministry of Education, Science, Technology, Sports and Culture, Japan; a grant from the Organization for Pharmaceutical Safety and Research, Japan; and a Health and Labor Sciences Research Grant from the Ministry of Health, Labor and Welfare, Japan.

[2] Address correspondence and reprint requests to Dr. Sachiko Hirose, Department of Pathology, Juntendo University School of Medicine, 2-1-1 Hongo, Bunkyo-ku, Tokyo 113-8421, Japan. E-mail address: sacchi@med.juntendo.ac.jp

[3] Abbreviations used in this paper: α-GalCer, α-galactosylceramide; SLE, systemic lupus erythematosus; B6, C57BL/6; NZB, New Zealand Black; NZW, New Zealand White; CIA, collagen-induced arthritis; QTL, quantitative trait loci; LOD, logarithm of odds; *Nim1*, NKT cell modifier 1; Tim, T cell Ig mucine.

In this context, the evidence of the role of NKT cells in SLE-prone (New Zealand Black (NZB) × New Zealand White (NZW))F_1 mice has been conflicting, with both suppressive and promoting roles having been reported (23, 29–32). As in cases of patients with SLE (11, 12), the age-associated reduction of NKT cells was reported to occur in (NZB × NZW)F_1 mice (23). However, there are also reports showing that the age-associated progression of (NZB × NZW)F_1 disease is associated with an expansion and activation of NKT cells (30, 32). Furthermore, the activation of NKT cells by repeated injections of α-GalCer in (NZB × NZW)F_1 mice was shown to exacerbate lupus nephritis (31), while treatment of (NZB × NZW)F_1 mice with anti-CD1d-blocking mAb ameliorated the disease (29, 31), suggesting that the role of NKT cells in these mice is disease promoting.

Early onset of severe SLE occurs in (NZB × NZW)F_1 mice under the control of multiple susceptibility and modifying alleles derived from both parental NZB and NZW strains (33). NZB mice are prone to autoimmune hemolytic anemia, and they also develop SLE, but the disease phenotypes are mild and develop much later in life compared with (NZB × NZW)F_1 mice. The NZW strain is principally a nonautoimmune strain, but it carries modifying genes to exacerbate SLE in the (NZB × NZW)F_1 hybrid. Our present study shows evidence that the potential of invariant TCR-bearing NKT cells to produce IL-4 and IFN-γ in response to α-GalCer is remarkably impaired in NZB mice, while such potential is highly up-regulated in NZW mice. This aberrant potential of NKT cells is genetically controlled, and the genetic element of NZW with the high producer phenotype is suggested to contribute to the exacerbation of SLE in the F_1 hybrid of NZB and NZW mice.

Materials and Methods

Mice

C57BL/6 (B6), BALB/c, NZB, NZW, and (NZB × NZW)F_1 mice, originally obtained from the Shizuoka Laboratory Animal Center (Shizuoka, Japan), were maintained in our animal facility. All mice were housed under identical conditions, and all experiments were performed in accordance with institutional guidelines. Female mice were used in this study.

Cell preparation

Single-cell suspensions from the spleen and liver were prepared by gently grinding the organs between the frosted ends of glass slides and filtering them through a 100-μm nylon mesh in RPMI 1640 (Sigma-Aldrich) containing 2% FCS (JRH Biosciences). Liver cells were subsequently resuspended in 40% isotonic Percoll solution, gently overlaid onto 80% isotonic Percoll solution, and centrifuged for 25 min at 2800 rpm at room temperature. Mononuclear cells were collected from the interface and washed once. RBC were lysed with an ammonium chloride lysis buffer and then washed once.

Flow cytometric analysis

To identify invariant TCR-bearing NKT cells, we used α-GalCer-loaded CD1d:Ig dimeric protein (Dimer XI, BD Pharmingen) consisting of the extracellular MHC class I-like domains of the mouse CD1d molecule fused with the V_H regions of mouse IgG1. To load α-GalCer onto the CD1d:Ig, the α-GalCer solution in DMSO was mixed with CD1d:Ig at 40 M excess of α-GalCer, and incubated at 37°C for 24 h. Aliquots of cells suspended in normal goat serum were incubated with α-GalCer-loaded CD1d:Ig at a final concentration of 0.1 μg/ml CD1d:Ig in 6.8% DMSO on ice for 60 min. Cells were washed once and stained with FITC-conjugated goat anti-mouse IgG on ice for 30 min. After washing and blocking nonspecific IgG-binding with 2.4G2 mAb, cells were further stained with allophycocyanin-conjugated anti-CD3 (2C11) mAb on ice for 30 min. For three-color flow cytometric analysis, cells were additionally stained with PE-conjugated anti-NK1.1 (PK136) on ice for 30 min. To analyze CD1d expression levels in a subpopulation of lymphocytes or to identify T cell, B cell, and NKT cell populations, aliquots of cells were double stained with appropriate combinations of the following mAbs: FITC-conjugated anti-CD3 (2C11), anti-CD11b (M1/70), anti-CD11c (HL3), anti-B220 (RA3.6B2), PE-conjugated anti-NK1.1, or Alexa Fluor 488-conjugated anti-CD1d (1B1) mAbs on ice for 30 min. After the cells were washed and fixed in PBS containing 0.2% BSA and 1% formaldehyde, stained cells in the lymphocyte gate, as determined by forward and side scattering, were analyzed using a FACStar^{Plus} flow cytometer and CellQuest software (BD Biosciences). α-GalCer was obtained from the Kirin Pharmaceutical Research Institute. Abs for flow cytometric analysis were all purchased from BD Pharmingen.

Isolation of lymphocyte subsets

Liver NKT cells were obtained by sorting α-GalCer-CD1d$^+$CD3$^+$ NKT cells using a FACSAria cell sorter (BD Biosciences). Splenic T cells were obtained by positive sorting of α-GalCer-CD1d$^-$CD3$^+$ T cells. T cell-depleted spleen cells (NKT and B cells) and NKT cell-depleted spleen cells (T and B cells) were obtained by negative sorting of α-GalCer-CD1d$^-$CD3$^+$ T cells and α-GalCer-CD1d$^+$CD3$^+$ NKT cells, respectively.

Measurement of Ag-presenting potential

The α-GalCer-presenting potential of splenic APCs was examined using NKT cell hybridoma, N38-3C3 (34). Spleen cells were treated with a mixture of rabbit complement (Cedarlane Laboratories) and Abs to Thy1.2 (J1J), CD4 (GK1.5), CD8 (53-6.7), and asialoGM1 (Wako Pure Chemical) to remove T, NK, and NKT cells and serve as a source of APCs. A mixture of 5×10^5 cells/well of APCs and 2×10^4 cells/well of hybridoma cells was cultured in a 96-well round-bottom plate for 2 days in RPMI 1640 culture medium supplemented with 10% FCS, 45 μM 2-ME (Sigma-Aldrich), 100 U/ml penicillin (Meiji Seika Kaisha), and 100 μg/ml streptomycin (Meiji Seika Kaisha) in the presence of several concentrations of α-GalCer. The potential for α-GalCer presentation was estimated by the measurement of IL-2 secreted into the culture supernatant by ELISA, as described below.

Assays for cytokine and Ig production

An aliquot of $\sim 1 \times 10^6$ cells/well, unless otherwise stated, was cultured in vitro in 96-well flat-bottom plates in RPMI 1640 culture medium for 2 days (for IL-4 and IFN-γ production) or 4 days (for Ig production). Cells were stimulated in a plate precoated with 10 μg/ml anti-CD3 (145–2C11) mAb or anti-CD3 and anti-CD28 (37.51) mAbs, or with a given concentration of α-GalCer. Levels of IL-2, IL-4, and IFN-γ in the culture supernatants were measured using standard sandwich ELISA with coated capture mAbs and biotinylated detection mAbs, according to the manufacturer's instructions (BD Pharmingen). Ig levels and anti-DNA Ab levels were measured using ELISA. Mouse IgG and IgM standards were purchased from Rockland. DNA-binding activities were expressed in units, referring to a standard curve obtained by serial dilution of a standard serum pool from (NZB × NZW)F_1 for 8 mo of age, containing 1000 U activities/ml.

Measurement of proteinuria

The severity of renal disease was monitored by biweekly testing for proteinuria, as described previously (35). Proteinuria was scored from grade 0 to 6, according to the amount of urinary albumin, in which 0 indicates <37 mg/100 ml; 1, ≥37 mg/100 ml; 2, ≥74 mg/ml; 3, ≥111 mg/100 ml; 4, ≥333 mg/100 ml; 5, ≥1000 mg/100 ml; and 6, ≥3000 mg/100 ml. Mice with urinary protein levels of 111 mg/100 ml or more in repeated tests were considered as being positive for proteinuria (35).

H-2 typing

H-2 typing was done by flow cytometry analysis using peripheral lymphocytes stained with FITC-conjugated anti-IA^u (Ia17) and anti-IA^d (m52) mAbs.

Genotyping

DNA was extracted from mouse-tail tissue. Genotyping for microsatellite markers was done using PCR. Microsatellite primers were purchased from Research Genetics. PCR reactions were run in a total volume of 20 μl containing 40 ng of genomic DNA. A three-temperature PCR protocol (94°C, 65°C, and 72°C) was used for 35 cycles in a GeneAmp 9600 thermal cycler (PerkinElmer-Cetus). PCR products were diluted 2-fold with loading buffer consisting of xylene cyanol and bromophenol blue dyes in 50% glycerin and were run on 18% polyacrylamide gels. After electrophoresis, bands were visualized by ethidium bromide staining.

Statistics

For analyses of mouse strain differences in the amounts of cytokines produced by NKT cells and of immunoglobulins by B cells, cell samples obtained from five to six mice from each strain were tested in three or five experiments, and the differences in the mean amounts ± SEM between mouse strains were analyzed by using the Mann-Whitney *U* test. In studies of backcross mice, the statistical analysis was also done using the Mann-Whitney *U* test ($p < 0.05$ was considered to be statistically significant). To estimate the positions of quantitative trait loci (QTL) for the amount of cytokine produced in vitro by α-GalCer-stimulated spleen cells, the likelihood ratio statistics were determined using the Map Manager QT package program. Logarithm of odds

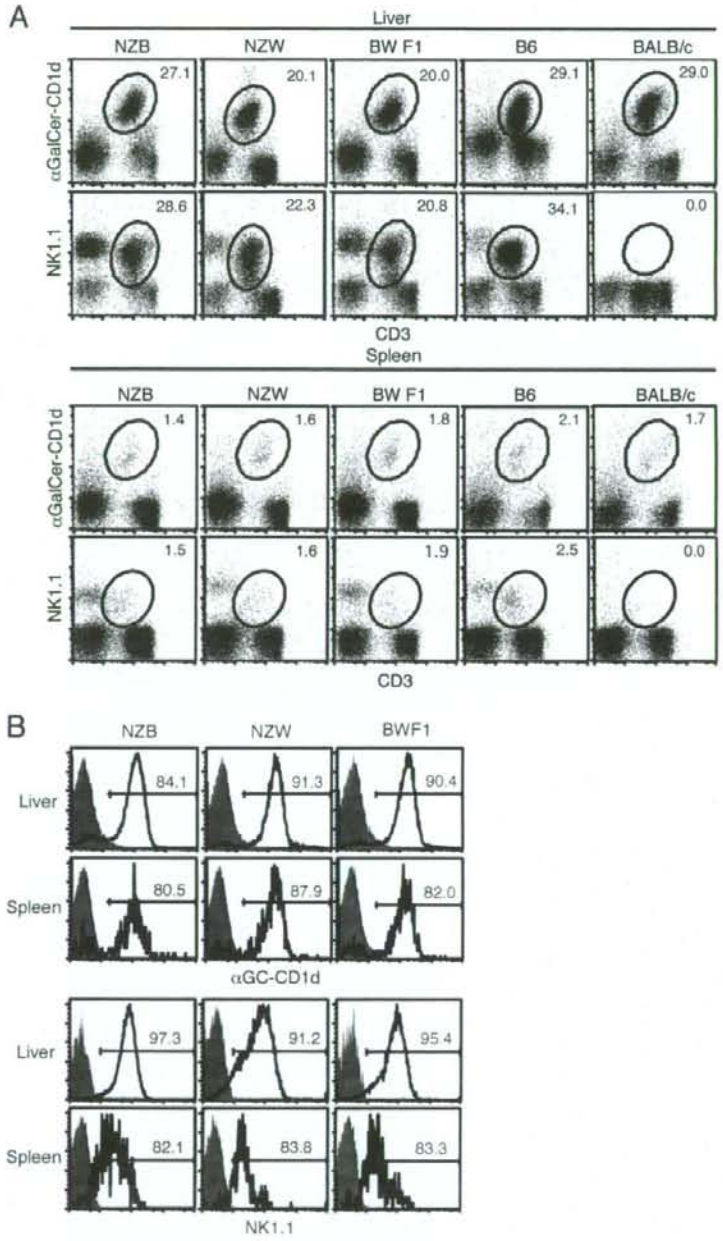

FIGURE 1. Representative flow cytometric analysis of NKT cells from livers and spleens of 2-mo-old NZB, NZW, (NZB × NZW) (BW) F_1, B6, and BALB/c mice. *A*, Double staining of liver mononuclear cells and spleen cells with anti-CD3 and α-GalCer-CD1d dimer or with anti-CD3 and anti-NK1.1 mAbs. Numbers show percentages of α-GalCer-CD1d$^+$CD3$^+$ NKT cells or NK1.1$^+$CD3$^+$ NKT cells per total of mononuclear cells shown in circles. Results are representative of five independent experiments. *B*, Analysis of α-GalCer-CD1d and NK1.1 expression on the surface of NK1.1$^+$ NKT cells and α-GalCer-CD1d$^+$ NKT cells, respectively. Liver mononuclear cells and spleen cells were triple stained with α-GalCer-CD1d, anti-CD3, and anti-NK1.1 mAbs, and α-GalCer-CD1d expression on NK1.1$^+$CD3$^+$ NKT cells and NK1.1 expression on α-GalCer-CD1d$^+$CD3$^+$ NKT cells were examined using histograms. The shaded histogram indicates the background staining. Numbers show percentage of α-GalCer-CD1d$^+$ and NK1.1$^+$ cells. Results are representative of three independent experiments.

(LOD) scores of ≥3.3 were used as the threshold for statistically significant linkage. In addition to the criteria using the fixed level of LOD, a permutation test for a significance level of 1% was also performed in 1-centiMorgan (cM) steps for 1000 permutations using the Map Manager QT package program to further estimate the significance levels for QTL analysis.

Results

Comparisons of the frequency and number of NKT cells among mouse strains

Frequencies of NKT cells in the livers and spleens of 2-mo-old NZB, NZW, (NZB × NZW)F_1, B6, and BALB/c mice were determined by double staining mononuclear cells with a mixture of anti-CD3 mAb and α-GalCer-loaded CD1d dimer or a mixture of anti-CD3 and anti-NK1.1 mAbs. The frequencies of α-GalCer-CD1d$^+$CD3$^+$ or NK1.1$^+$CD3$^+$ NKT cells were higher in the liver as compared with those seen in the spleen (BALB/c mice are negative for the NK1.1 allele) (Fig. 1*A*). The NKT cell frequencies in the livers of NZW and (NZB × NZW)F_1 mice tended to be lower than those in other mouse strains; however, there was no statistically significant strain difference in α-GalCer-CD1d$^+$CD3$^+$ NKT cell frequencies in either spleens or livers (Table I). In flow cytometric analysis using cells triple stained with anti-CD3 mAb, anti-NK1.1 mAb, and α-GalCer-CD1d dimer, >80% of the NK1.1$^+$CD3$^+$ NKT cells in the livers and spleens of NZB, NZW, and (NZB × NZW)F_1 mice were α-GalCer-CD1d$^+$ (Fig. 1*B*), and >90% of α-GalCer-CD1d$^+$CD3$^+$ NKT cells in livers

Table I. *Frequency and number of α-GalCer-CD1d$^+$CD3$^+$ NKT cells*

	NZB	NZW	BW F_1	B6	BALB/c
Frequency in livers (%)					
2-mo-old	27.8 ± 2.3	20.3 ± 6.2	23.3 ± 3.7	29.1 ± 1.0	29.0 ± 2.0
8-mo-old	31.1 ± 9.9	21.2 ± 0.3	24.5 ± 0.3	ND	ND
Frequency in spleens (%)					
2-mo-old	1.4 ± 0.2	1.7 ± 0.2	2.0 ± 0.2	2.1 ± 0.1	1.8 ± 0.2
8-mo-old	2.4 ± 0.4	2.4 ± 0.3	1.8 ± 0.3	ND	ND
Total NKT cell number in spleens ($\times 10^5$)					
2-mo-old	1.1 ± 0.2	1.3 ± 0.4	1.6 ± 0.5	2.1 ± 0.3	2.0 ± 0.2
8-mo-old	4.3 ± 0.6[a]	2.4 ± 0.8	5.5 ± 1.9[a]	ND	ND

Data show mean ± SEM of 5–8 mice.
[a] Significantly increased compared to the number of 2-mo-old mice ($p < 0.05$).

expressed high levels of NK1.1 Ag. A notable finding was that although >80% of α-GalCer-CD1d$^+$CD3$^+$ NKT cells in spleens were also NK1.1$^+$, the expression levels of NK1.1 Ag were remarkably reduced in spleens, as compared with those in livers (Fig. 1*B*), and the findings were consistent with a previous report (32).

We then examined the age-associated changes in the frequency of α-GalCer-CD1d$^+$CD3$^+$ NKT cells in New Zealand mouse strains. As shown in Table I, comparisons of NKT cell frequencies between 2- and 8-mo-old NZB, NZW, and (NZB × NZW)F_1 mice showed that there were no age-associated changes in either livers or spleens. However, when the total number of NKT cells in spleens was compared, a significant age-associated increase was observed in enlarged spleens from older NZB and (NZB × NZW)F_1 mice.

Comparisons of cytokine-producing potential of NKT cells among mouse strains

We then compared the in vitro cytokine-producing potential of spleen cells upon stimulation with varying concentrations of α-GalCer among 2-mo-old NZB, NZW, (NZB × NZW)F_1, B6, and BALB/c mice. As shown in Fig. 2*A*, spleen cells responded to

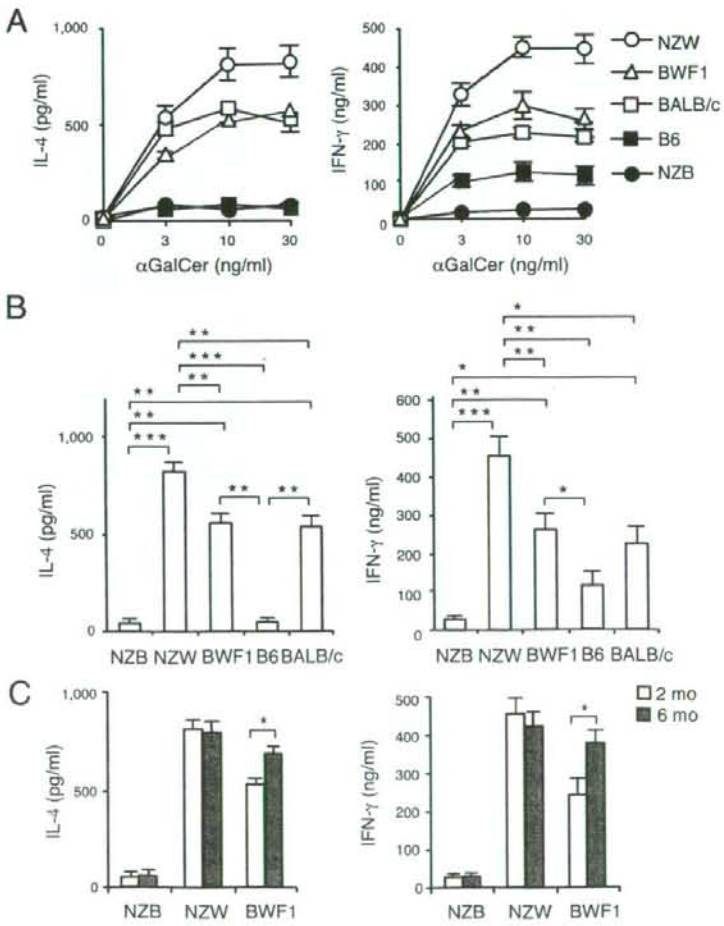

FIGURE 2. Comparison of in vitro IL-4- and IFN-γ-producing potential of α-GalCer-stimulated spleen cells among mouse strains. *A*, Comparison of the potential among 2-mo-old mice. Whole spleen cells in triplicate cultures were cultured for 2 days in the presence of varying concentrations of α-GalCer, and the concentrations of IL-4 and IFN-γ in the culture supernatants were measured by ELISA. The mean amounts ± SEM of cytokines show data obtained from 5–6 mice from each strain in triplicate experiments. *B*, Spleen cells from 2-mo-old mice were cultured for 2 days in the presence α-GalCer (30 ng/ml), and the concentrations of IL-4 and IFN-γ in the culture supernatants were measured by ELISA. The mean amounts ± SEM of cytokines show data obtained from 5–6 mice from each strain in triplicate experiments. ***, $p < 0.001$; **, $p < 0.01$; and *, $p < 0.05$. *C*, Age-associated changes in cytokine producing potential of α-GalCer-stimulated spleen cells. Whole spleen cells from 2- and 6-mo-old NZB, NZW, and BW F_1 mice were cultured for 2 days in the presence of 30 ng/ml α-GalCer, and the concentrations of IL-4 and IFN-γ in the culture supernatants were measured by ELISA. The mean amounts ± SEM of cytokines show data obtained from 5–6 mice from each strain at 2 and 6 mo of age in triplicate experiments. *, $p < 0.05$.

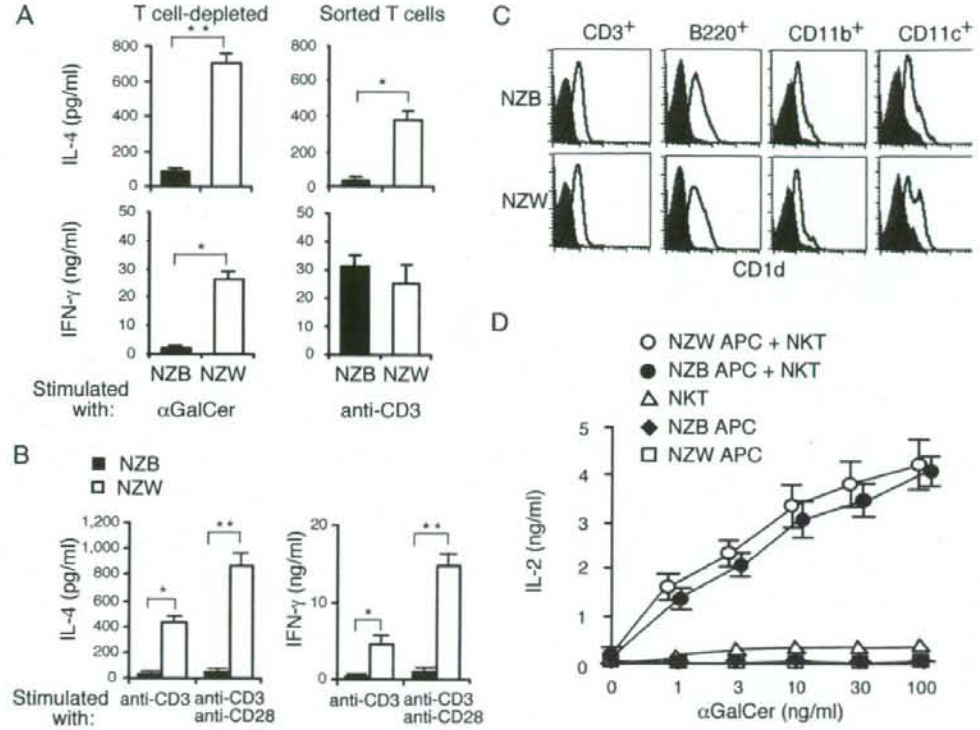

FIGURE 3. Evidence that aberration in cytokine-producing potential of α-GalCer-stimulated spleen and liver cells from New Zealand mice is attributed to NKT cells per se. *A*, Comparison of in vitro IL-4- and IFN-γ-producing potential of α-GalCer-stimulated T cell-depleted spleen cells and anti-CD3 mAb-stimulated FACS-sorted splenic T cells between NZB and NZW mice. Spleen cells from 2-mo-old mice were stained with α-GalCer-CD1d and anti-CD3 mAb, and T cell-depleted spleen cells and splenic T cells were obtained by negative and positive sorting of α-GalCer-CD1d$^-$CD3$^+$ T cells, respectively. The purity of the cells was 99% in these experiments. Sorted cells (1×10^6 cells/well) were cultured for 2 days in the presence of α-GalCer (30 ng/ml) or immobilized anti-CD3 mAb (10 μg/ml), and the concentrations of IL-4 and IFN-γ in the culture supernatants were measured by ELISA. The mean amounts ± SEM of cytokines show data from 5 mice from each strain in five experiments. **, $p < 0.001$; and *, $p < 0.01$. *B*, Comparison of cytokine-producing potential of flow cytometry-sorted liver NKT cells between NZB and NZW mice in response to immobilized anti-CD3 mAb and to anti-CD3 plus anti-CD28 mAbs. Liver NKT cells were obtained by positive sorting of α-GalCer-CD1d$^+$CD3$^+$ NKT cells from 2-mo-old NZB and NZW mice. The purity of the cells was >96% in both NZB and NZW experiments. Flow cytometry-sorted cells (2×10^5 cells/well) were cultured for 2 days in a plate precoated with anti-CD3 mAb (10 μg/ml) or with anti-CD3 and anti-CD28 (10 μg/ml) mAbs, and the concentrations of IL-4 and IFN-γ in the culture supernatants were measured by ELISA. The mean amounts ± SEM of cytokines show data from 5 mice from each strain in five experiments. **, $p < 0.001$; and *, $p < 0.01$. *C*, Comparison of CD1d expression levels on the surface of splenic CD3$^+$ T cells, B220$^+$ B cells, CD11b$^+$ macrophages, and CD11c$^+$ dendritic cells by histogram between 2-mo-old NZB and NZW mice. Results are representative of three independent experiments. The shaded histogram indicates the background staining. *D*, Comparison of α-GalCer-presenting potential of APCs to NKT hybridoma cells (N38-3C3) between NZB and NZW mice. APCs were prepared from spleen cells of 2-mo-old mice by complement-dependent lysis of cells using Abs to Thy1.2, CD4, CD8, and asialoGM1, and cultured with or without NKT hybridoma cells (N38-3C3) in the presence of α-GalCer. α-GalCer-presenting potential was estimated by measurement of IL-2 produced by NKT hybridoma cells in culture. The concentration of IL-2 was measured by ELISA. The mean amounts ± SEM of cytokines show data from 5–6 mice from each strain in triplicate experiments.

α-GalCer in a dose-dependent manner; however, levels of the potential to produce IL-4 and IFN-γ varied considerably among the mouse strains. Spleen cells from BALB/c mice produced considerable amounts of both IL-4 and IFN-γ, while those from B6 mice produced a significant amount of IFN-γ but a minimal amount of IL-4. Intriguingly, compared with the findings in B6 and BALB/c mice, spleen cells from NZW mice produced larger amounts of both IL-4 and IFN-γ. In contrast, NZB spleen cells produced minimal amounts of both IL-4 and IFN-γ, and the amounts of IL-4 and IFN-γ produced by (NZB × NZW)F_1 spleen cells were intermediate between the parental NZW and NZB mice. Fig. 2*B* compares IL-4- and IFN-γ-producing potentials of spleen cells stimulated with 30 ng/ml α-GalCer among mouse strains. NZW spleen cells produced significantly larger amounts of IL-4 and IFN-γ than those from other mouse strains tested. In contrast, NZB spleen cells produced significantly smaller amounts of both cytokines, as compared with those from NZW, (NZB × NZW)F_1, and BALB/c mice.

We next examined age-associated changes in cytokine-producing potential of α-GalCer-stimulated spleen cells from NZB, NZW, and (NZB × NZW)F_1 mice (Fig. 2*C*). Although spleen cells from NZB and NZW mice showed no significant changes, there was a significant age-associated increase in potential to produce both IL-4 and IFN-γ by spleen cells from (NZB × NZW)F_1 mice.

To see whether such aberrant cytokine-producing potential of α-GalCer-stimulated spleen cells from NZB and NZW mice is indeed attributed to NKT, but not T cells, T cell-depleted spleen cells were stimulated in vitro in the presence of α-GalCer, and the amounts of IL-4 and IFN-γ produced were examined. As shown in Fig. 3*A*, while T cell-depleted spleen cells from NZW mice

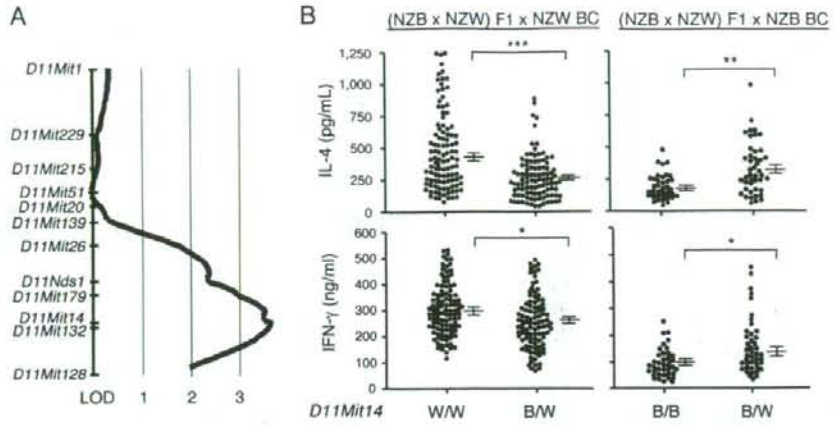

FIGURE 4. Locus controlling cytokine-producing potential of NKT cells. *A*, QTL scan of chromosome 11 for the amount of IL-4 produced in vitro by αGalCel-stimulated spleen cells in 205 (NZB × NZW)F_1 × NZW backcross mice. The LOD score curve is shown on the right with the scale on the bottom. Map positions of microsatellite markers are arranged from the centromere to the telomere on the left of the chromosome line. *B*, Correlation of the amounts of IL-4 and IFN-γ produced by α-GalCer-stimulated spleen cells with NZW-derived *D11Mit14* genotype in 205 (NZB × NZW)F_1 × NZW and 83 (NZB × NZW)F_1 × NZB backcross mice. Spleen cells from 2-mo-old backcross mice were cultured for 2 days in the presence of α-GalCer (30 ng/ml), and the concentrations of IL-4 and IFN-γ in the culture supernatants were measured by ELISA. The results of individual mice are shown as dots, and the mean ± SEM is shown on the right side. W/W, B/W, and B/B represent NZW/NZW, NZB/NZW, and NZB/NZB genotypes, respectively, for the *D11Mit14* microsatellite marker. ***, $p < 0.001$; **, $p < 0.01$; and *, $p < 0.05$.

produced significant amounts of both cytokines, only limited amounts of both cytokines were produced by those from NZB mice. Fig. 3*A* also shows the potential of FACS-sorted T cells from NZB and NZW mice to produce IL-4 and IFN-γ in response to immobilized anti-CD3 mAb. As for the production of IL-4, a significant amount was produced by NZW T cells and a limited amount by NZB T cells, similar to the profile of IL-4 synthesis by NKT cells. However, the IFN-γ-producing potential of T cells differed markedly from that of NKT cells, in which NZB T cells produced comparable amounts of IFN-γ as NZW T cells did.

Because the functional deficiency of NKT cells from NZB mice was remarkable, we then examined whether the functional defect in NZB NKT cells is due to NKT cells per se or to the impaired Ag-presenting potential of CD1d-bearing APCs. To exclude the effect of APCs, we first sorted α-GalCer-CD1d$^+$CD3$^+$ liver NKT cells, stimulated with immobilized anti-CD3 mAb alone or together with mAb against costimulatory molecule CD28, and measured the amounts of IL-4 and IFN-γ in the culture supernatants. As shown in Fig. 3*B*, NZB NKT cells produced minimal amounts of both IL-4 and IFN-γ even in the presence of anti-CD3 and anti-CD28 mAbs, compared with NZW NKT cells that produced large amounts of both cytokines, suggesting that the functional deficiency of NZB NKT cells is intrinsic. To confirm this notion, we then compared CD1d expression levels on the surfaces of immune cells and the potential of APCs to present α-GalCer to NKT cells between NZB and NZW mice. Fig. 3*C* shows that there were no differences in CD1d expression levels on CD3$^+$ T cells, B220$^+$ B cells, CD11b$^+$ macrophages, or CD11c$^+$ dendritic cells between NZB and NZW mice. To compare the potential of APCs to present α-GalCer, the APC-rich cell suspension, obtained by depletion of T cells, NK cells, and NKT cells using complement-dependent lysis of spleen cells with Abs to Thy1.2, CD4, CD8, and asialoGM1, were cocultured with the cell suspension of an NKT hybridoma cell line, N38–3C3 (34), in the presence of varying concentrations of α-GalCer. As shown in Fig. 3*D*, APCs from both NZW and NZB mice were able to present α-GalCer to the NKT hybridoma cells, as estimated by IL-2 levels produced by the hybridoma cells.

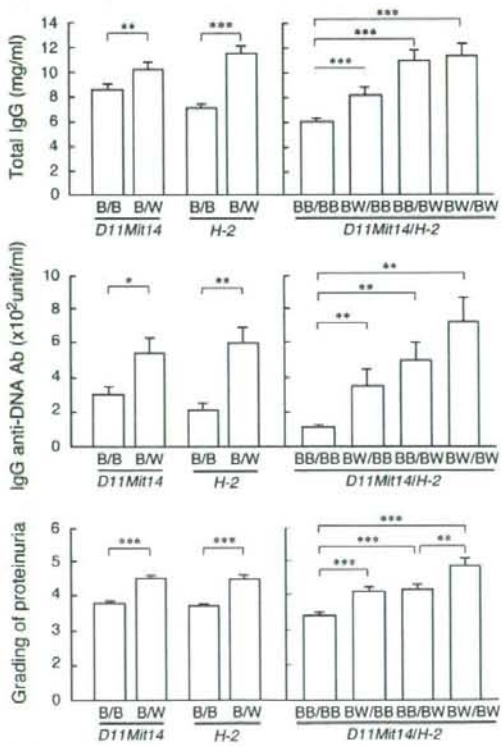

FIGURE 5. Correlation of high serum levels of total IgG, IgG anti-DNA Abs, and severity of proteinuria with the NZW-derived *D11Mit14* genotype and *H-2* haplotype in 262 (NZB × NZW)F_1 × NZB backcross mice. Backcross mice were divided into two or four groups according to *D11Mit14* genotype, *H-2* haplotype, or the combination of both, and disease phenotypes were compared at 8 mo of age among each group. Data represent the means ± SEM. ***, $p < 0.001$; **, $p < 0.01$; and *, $p < 0.05$.

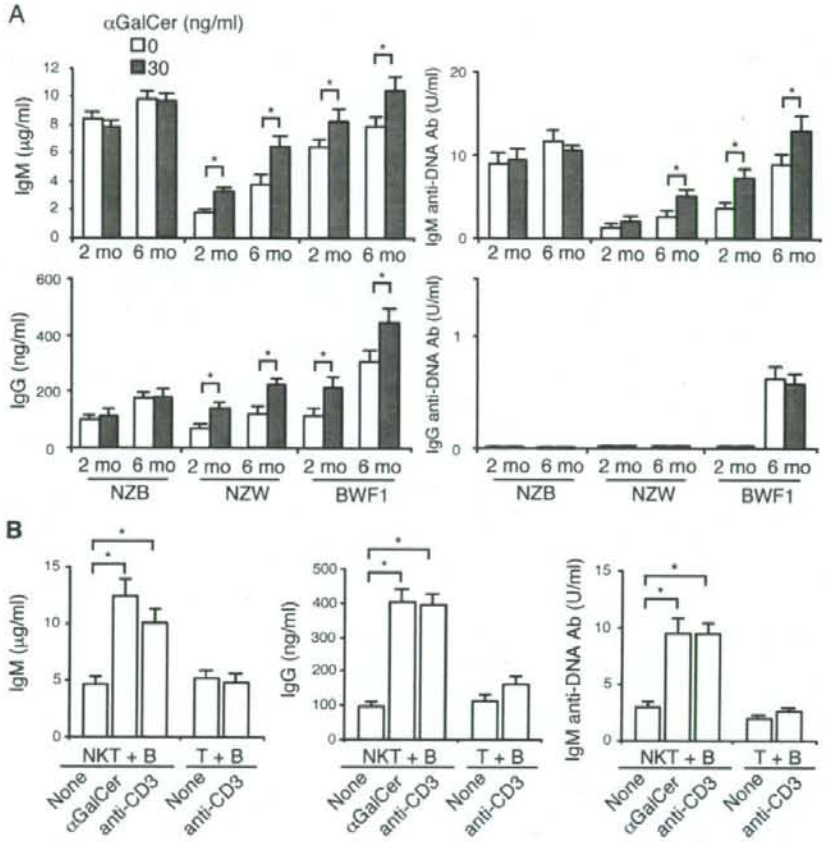

FIGURE 6. Effect of α-GalCer stimulation of spleen cells on Ig synthesis. *A*, Comparison of the potential of α-GalCer-stimulated spleen cells to help Ig synthesis in vitro among NZB, NZW, and (NZB × NZW) (BW) F_1 mice. Spleen cells from 2- and 6-mo-old mice were cultured (1×10^6 cells/well) for 4 days in the presence or absence of α-GalCer, and the amounts of total IgM and IgG, and IgM and IgG anti-DNA Abs in the culture supernatants were measured by ELISA. The mean amounts ± SEM of immunoglobulins show data from 5–6 mice from each strain at 2 and 6 mo of age in triplicate experiments. *, $p < 0.05$. *B*, NKT cell-mediated augmentation of Ig synthesis. Spleen cells from 6-mo-old BW F_1 mice were stained with α-GalCer-CD1d and anti-CD3 mAb, and T cell-depleted spleen cells (NKT + B) and NKT cell-depleted spleen cells (T + B) were prepared by negative sorting of α-GalCer-CD1d$^-$CD3$^+$ T cells and of α-GalCer-CD1d$^+$CD3$^+$ NKT cells, respectively. The purity of the sorted cells was 99% in both populations. The populations of NKT + B cells (5×10^5 cells/well) and of T + B cells (1×10^6 cells/well) were cultured for 4 days in the presence or absence of α-GalCer (30 ng/ml) or anti-CD3 mAb, and the amounts of total IgM and IgG, and IgM anti-DNA Abs in the culture supernatants were measured by ELISA. The mean amounts ± SEM of immunoglobulins show data from 5 mice from each strain in five experiments. *, $p < 0.05$.

Locus controlling cytokine production by NKT cells

To identify the genetic locus controlling in vitro cytokine production by α-GalCer-stimulated NKT cells, a genome-wide QTL analysis was performed using 108 microsatellite markers in 205 (NZB × NZW)F_1 × NZW backcross mice at 2 mo of age. As shown in Fig. 4*A*, we identified one QTL for the high IL-4-producing phenotype tightly linked to the microsatellite marker *D11Mit14* (57 cM from the centromere: map position in Mouse Genome Informatics database) on NZW chromosome 11 with significant linkage (LOD of 3.6). To further estimate the significance level of this linkage, a permutation test was performed. The result showed that the likelihood ratio statistic value was 17.2, a figure higher than the critical value of significant linkage (12.6).

In these backcross mice, the group of progeny with the NZW/NZW (W/W) genotype for *D11Mit14* showed significantly higher levels of not only IL-4 but also IFN-γ than did the progeny with the NZB/NZW (B/W) genotype for *D11Mit14* (Fig. 4*B*), suggesting that the *D11Mit14*-linked NZW locus is also involved in the up-regulation of IFN-γ-producing potential of NKT cells. This was supported by studies using 83 (NZB × NZW)F_1 × NZB backcross mice, in which the group of progeny with the NZB/NZW (B/W) genotype for *D11Mit14* showed significantly higher levels of not only IL-4 but also IFN-γ than did the progeny with the NZB/NZB (B/B) genotype for *D11Mit14* (Fig. 4*B*).

Correlation between the genotype for D11Mit14 and SLE phenotypes

To determine whether the *D11Mit14*-linked NZW locus contributes to SLE susceptibility, the correlation between *D11Mit14* genotype and serum levels of total IgG, IgG anti-DNA Abs, and the severity of proteinuria was examined using 262 8-mo-old (NZB × NZW)F_1 × NZB backcross mice. As shown in Fig. 5, the progeny with the NZB/NZW (B/W) genotype for *D11Mit14* showed significantly higher serum levels of total IgG and IgG anti-DNA Abs and developed more severe proteinuria than did the progeny with the NZB/NZB (B/B) genotype.

As we reported previously (36–38), the *H-2* haplotype is an important genetic element for severe SLE in (NZB × NZW)F_1

mice. This was evident in studies of backcross progeny, in which *H-2* heterozygous progeny (B/W:$H\text{-}2^{d/z}$) showed much more severe SLE phenotypes than did the *H-2* homozygotes (B/B:$H\text{-}2^{d/d}$). To assess interactions of the *D11Mit14*-linked locus and the *H-2* haplotype, we divided backcross mice into four groups according to *D11Mit14* genotype and *H-2* haplotype and compared the disease severity. The ANOVA suggested that the *D11Mit14*-linked NZW locus and $H\text{-}2^{d/z}$ heterozygosity appear to play roles in exacerbation of (NZB × NZW)F_1 disease in an additive manner (Fig. 5).

Effect of α-GalCer-stimulated NKT cells on Ig synthesis

To investigate the mechanism that underlies the correlation between the *D11Mit14* genotype and serum autoantibody levels in studies of the backcross progeny, we examined the effect of α-GalCer-stimulated NKT cells on Ig synthesis by B cells. Spleen cells from 2- and 6-mo-old NZB, NZW, and (NZB × NZW)F_1 mice were cultured in vitro in the presence or absence of α-GalCer, and Ig levels in the culture supernatants were examined. As shown in Fig. 6*A*, the addition of α-GalCer to the cell cultures significantly enhanced IgM, IgG, and IgM anti-DNA Ab synthesis in NZW and (NZB × NZW)F_1 mice, but not in NZB mice. A small but significant amount of IgG anti-DNA Abs was detected in spleen cell cultures of 6-mo-old (NZB × NZW)F_1 mice; however, α-GalCer-stimulation showed no enhancing effect.

To clarify that such up-regulation of Ig synthesis is due to the activation of NKT cells, we obtained T cell-depleted spleen cells (NKT + B) by negative sorting of α-GalCer-$CD1d^-CD3^+$ T cells and NKT cell-depleted spleen cells (T + B) by negative sorting of α-GalCer-$CD1d^+CD3^+$ NKT cells from 6-mo-old (NZB × NZW)F_1 mice, and cultured them in the absence or presence of either α-GalCer or immobilized anti-CD3 mAb. The production of IgM, IgG, and IgM anti-DNA Abs was up-regulated in cultures of NKT + B cells in the presence of α-GalCer or anti-CD3 mAb, but not in cultures of T + B cells in the presence of anti-CD3 mAb (Fig. 6*B*). The amount of IgG anti-DNA Abs was below the detectable level in this culture system (data not shown). These findings may support the view that the α-GalCer-mediated up-regulation of Ig synthesis by B cells is not due to the effect of *trans*-activated T cells.

Discussion

In the present study, we found that although NZB and NZW mice have normal frequencies of invariant TCR-bearing NKT cells, their potentials for cytokine production were remarkably different. Upon stimulation with α-GalCer, NKT cells from NZB mice were defective in producing both IL-4 and IFN-γ, while such potential of NKT cells in NZW mice was highly up-regulated. The cytokine production level of F_1 hybrid progeny of NZB and NZW was intermediate. As the mode of cytokine production differed between NKT cells and T cells, these two types of cells appear to be under the control of separate mechanisms.

Because the aberrant cytokine-producing potential of NKT cells in New Zealand strains of mice was evident in young mice before the onset of immunological abnormalities, certain genetic mechanisms were thought to underlie this aberration. Genome-wide QTL analysis mapped one significant locus tightly linked to a microsatellite marker, *D11Mit14* (57 cM from the centromere), on telomeric chromosome 11 for controlling IL-4 synthesis by α-GalCer-stimulated spleen cells. The significance of this locus, provisionally designated *Ntm1* (NKT cell modifier 1) in this paper, was supported by findings in progeny studies, indicating that the *D11Mit14* genotype of the NZW strain correlated significantly with the elevated potential of α-GalCer-stimulated spleen cells to produce IL-4. Although QTL analysis for IFN-γ production did not show a significant linkage, the association studies suggested that the *D11Mit14* is also involved in the control of IFN-γ production by NKT cells. The significance levels of the difference in IFN-γ production between W/W and B/W and between B/B and B/W for the *D11Mit14* genotype in the backcross progeny were lower than the levels in IL-4 production in backcross studies. Thus, it is conceivable that the genetic control of IFN-γ production by α-CalCer-stimulated NKT cells is more complex than that of IL-4, involving an additional locus or loci. Further genetic analysis is required to solve this issue.

Matsuki et al. (39) reported that the number and function of invariant TCR-bearing NKT cells in type I diabetes-prone NOD mice are regulated by several genes, including a gene (or genes) located in the *Idd4* interval on chromosome 11. These authors showed that congenic B6 mice bearing NOD-*Idd4* had reduced numbers of hepatic invariant NKT cells, resulting in a reduced cytokine response following in vivo activation with α-GalCer (39). This *Idd4* interval covers a broad segment, including the *D11Mit14*-linked *Ntm1* locus. At present, the genes in the *Idd4* and *Ntm1* loci are as yet unidentified. In the vicinity of *D11Mit14*, there is a gene for G-CSF (57 cM from the centromere). It is known that NKT cells express receptors for G-CSF (40). Crough et al. (41) reported that administration of G-CSF results in polarization of NKT cells toward a Th2 cytokine-secreting phenotype following α-GalCer stimulation. Thus, G-CSF may have the potential to influence cytokine production by NKT cells. However, α-GalCer-stimulated NZW and NZB NKT cells did not polarize to either Th1 or Th2 cytokine-producing phenotypes in the present study. Furthermore, because the aberrant cytokine-producing phenotypes in NZB and NZW NKT cells are intrinsic to NKT cells per se, the G-CSF gene itself may not be the gene under investigation.

Since Th1/Th2 balance is critical in immune regulation, it is important to determine its correlation to the underlying mechanism controlling cytokine production by NKT cells. In the regulation of $CD4^+$ Th1/Th2 cells, Gorham et al. (42) mapped a locus, *Tpm1* (T cell phenotype modifier 1), to the middle region on chromosome 11, using crosses of Th1-polarized B10.D2 and Th2-polarized BALB/c strains. This interval contains several potent candidate genes, such as genes for IL-4 and IFN regulatory factor-1, both of which are mapped at 29 cM from the centromere. Another molecule possibly involved in the regulation of Th1/Th2 balance of $CD4^+$ T cells are T cell membrane proteins encoded by *Tim* (T cell Ig mucine) family genes (43, 44). Th1 and Th2 cells express Tim-3 and Tim-1, respectively, and the interaction of Tim proteins and their ligands is suggested to be involved in Th1/Th2 balance. Tim genes are located 5–10 cM upstream from *Tpm1* (42) on chromosome 11. Thus, both *Tpm1* and *Tim* genes are not linked to the *D11Mit14*-linked locus *Ntm1* for NKT cells. Together with our present findings that the mode of cytokine production differs between T cells and NKT cells in New Zealand mice, it seems likely that separate genetic mechanisms are involved in the control of their cytokine-producing potential between T cells and NKT cells. In support of this view, we found recently that the in vitro IL-producing potential of naive T cells is tightly linked to the polymorphic IL-4Rα-chain gene on chromosome 7 (45).

Zeng et al. (31) reported that activation of NKT cells following in vivo administration of α-GalCer in (NZB × NZW)F_1 mice induces Th1-type immune responses that exacerbate SLE in these mice. Studies by Forestier et al. (32) indicated that the development of SLE in (NZB × NZW)F_1 mice was associated with an expansion and activation of NKT cells, and that activation of NKT cells in these mice in vivo or in vitro with α-GalCer revealed a marked increase in their potential to contribute to the production of

IFN-γ with advancing age and disease progression. These findings may support the notion that NKT cells in (NZB × NZW)F_1 mice play a promoting, rather than a suppressive, role in the pathogenesis of SLE. The results of our present study are consistent with this notion; however, several points require discussion. First, NKT cells from (NZB × NZW)F_1 and NZB mice showed a significant age-associated increase; however, our results showed that they did not undergo proportional expansion. This may be because we only examined the mice at 2 and 8 mo of age. Forestier et al. (32) indicated that in the spleens from aged (NZB × NZW)F_1 mice, because of the remarkable hypercellularity that developed in this organ during the progression of SLE, expansion of the total number of NKT cells was not reflected as proportional expansion. These authors showed evidence that both the percentage and the absolute number of NKT cells are increased in the spleen of mice at 14 wk of age, a time when these mice have not yet developed significant disease phenotypes. Because invariant TCR-bearing NKT cells are self-reactive (46) and recognize lysosomal isoglobotrihexosylceramide (iGb3), a potent endogenous ligand for NKT cell activation (47), it seems feasible that NKT cells may expand in response to large amounts of such ligands released from apoptotic cells as inflammatory tissue injuries progress in a wide variety of tissues in older (NZB × NZW)F_1 mice. In contrast, NZB mice are prone to autoimmune hemolytic anemia and also spontaneously develop splenomegaly as animals age (33). In our present study, although they showed age-associated increases in the number of NKT cells in their enlarged spleens, these NKT cells, like those from young mice, produced minimal amounts of IL-4 and IFN-γ in response to α-GalCer. These findings also support our notion that NZB-type *Ntm1* is defective, and thus different mechanisms are suggested to underlie the pathogenesis of autoimmune disease in NZB mice.

Second, our study shows evidence that α-GalCer-stimulated NKT cells in (NZB × NZW)F_1 mice produce considerable amounts of both IFN-γ and IL-4 even in mice at older ages, and the cytokine profile did not polarize to IFN-γ. As our research was limited to the in vitro responses of NKT cells to α-GalCer, further in vivo studies may be necessary to reach a definitive conclusion. To clarify further whether the aberrant NKT cell functions found in the in vitro studies are indeed involved in the pathogenesis of SLE in NZB/WF_1 mice, we are now on the way to establishing interval congenic New Zealand mouse strains carrying either the NZB-type or NZW-type allele for the *D11Mit14* genotype. Taking advantage of these congenic strains, we intend to analyze the mechanism of the role of *D11Mit14*-linked alleles in aberrant NKT cell functions and the mechanisms of their contribution to SLE pathogenesis. Recently, NKT cells were found to produce additional cytokines such as IL-13 (48) and IL-21 (49). It will be interesting to see whether the *D11Mit14*-linked locus also regulates the production of these cytokines and whether their changes influence SLE phenotypes in (NZB × NZW)F_1 mice.

The NZW genotype for *D11Mit14* correlates significantly with the serum levels of IgG, IgG anti-DNA Abs, and the severity of proteinuria in (NZB × NZW)F_1 × NZB backcross progeny, suggesting that the *Ntm1* locus-mediated NKT cell function is linked to the (NZB × NZW)F_1 disease. The present in vitro studies demonstrated that, upon stimulation with α-GalCer, NKT cells from NZW and (NZB × NZW)F_1 mice, but not NZB mice, were able to promote polyclonal IgM, IgG, and IgM anti-DNA Ab production by B cells. These findings are consistent with the report of Forestier et al. (32), indicating that anti-CD3 mAb-stimulated CD1d-restricted NKT cells derived from (NZB × NZW)F_1 mice are able to strongly augment B cell activation in vitro, as determined by polyclonal B cell proliferation and secretion of Igs. Intriguingly, NKT cells from older (NZB × NZW)F_1 mice injected under the renal capsule in young F_1 mice enhanced the injury in renal glomeruli (30). The underlying mechanism for the up-regulated Ig synthesis mediated by activated NKT cells remains undetermined. Our preliminary studies showed that this event occurs in the absence of cognate interaction between B and NKT cells; however, addition of IL-4, IFN-γ, or a combination of both failed to augment Ig synthesis (data not shown), suggesting the involvement of other factors. In this respect, IL-21 is of particular importance, because this cytokine is produced by NKT cells and shows pleiotropic effects on the functions of several types of immune cells, including B cells (49).

Although NKT cells did promote polyclonal IgG syntheses in vitro by B cells from older (NZB × NZW)F_1 mice, they did not promote the IgG anti-DNA Ab synthesis. There are two possible explanations. First, self-reactive B cells in older (NZB × NZW)F_1 mice are already activated in vivo, and thus are unresponsive to additional activators. Our earlier findings may be relevant that while B cells from young (NZB × NZW)F_1 mice showed high proliferative responses to IL-2, B cells from older mice were unresponsive (50). Alternatively, NKT cells alone cannot provide signals for affinity maturation of anti-DNA B cells. We have reported previously that MHC class II haplotype heterozygosity, one derived from NZB ($H\text{-}2^d$) and the other from NZW ($H\text{-}2^z$), is a critical genetic element for severe SLE in (NZB × NZW)F_1 mice (36–38) through a mechanism that mediates IgM to IgG class switching and affinity selection of pathogenic self-reactive B cells (51, 52). Because this process requires both $CD4^+$ Th cells and self-Ag, *MHC class II* genes are thought to serve as a genetic element for the production of Ag-specific high-affinity IgG autoantibodies. Together with the findings in genetic studies that the effects of the NZW-type *H-2* haplotype and *Ntm1* are cooperative in the production of pathogenic IgG anti-DNA Abs in (NZB × NZW)F_1 mice, it is highly likely that the NZW-type *Ntm1* contributes to the production of such pathogenic autoantibodies by stimulating polyclonal B cells, including anti-DNA B cells, to be susceptible to signals from MHC class II-restricted $CD4^+$ anti-DNA Th cells. Thus, the NZW *Ntm1* allele is considered to be a candidate SLE modifier that acts to exacerbate disease in (NZB × NZW)F_1 mice. Conversely, the defect in NZB *Ntm1* may be related in part to the delayed onset of mild SLE in these mice. Indeed, there is evidence that the event of IgM to IgG class switching of anti-DNA Abs occurs much less in NZB than in (NZB × NZW)F_1 mice (33).

Accumulated evidence showed that NKT cells are a crossroad between innate immunity and adaptive immunity. Although autoimmune disease is Ag-driven, NKT cells may be involved in the modulation of disease phenotypes, in either promoting or protective roles. Mechanisms that lead to the difference in roles of NKT cells in autoimmune diseases are not clearly understood. Further studies on the genetic mechanisms of cytokine regulation in NKT cells may contribute to a more thorough understanding of their roles in a variety of autoimmune diseases.

Acknowledgments

We thank Drs. T. Yamamura and S. Miyake (National Institute of Neuroscience) for helpful discussions.

Disclosures

The authors have no financial conflicts of interest.

References

1. Bendelac, A., M. N. Rivera, S. H. Park, and J. K. Roark. 1997. Mouse CD1d-specific $NK1.1^+$ T cells: development, specificity, and function. *Annu. Rev. Immunol.* 15: 535–562.

2. Porcelli, S. A., and R. L. Modlin. 1999. The CD1d system: antigen presenting molecules for T cell recognition of lipids and glycolipids. *Annu. Rev. Immunol.* 17: 297–329.
3. Kronenberg, M., and L. Gapin. 2002. The unconventional lifestyle of NKT cells. *Nat. Rev. Immunol.* 2: 557–568.
4. Taniguchi, M., N. Harada, S. Koji, T. Nakayama, and H. Wakao. 2003. The regulatory role of Vα14 NKT cells in innate and acquired immune response. *Annu. Rev. Immunol.* 21: 483–513.
5. Brigl, M., and M. B. Brenner. 2004. CD1: antigen presentation and T cell function. *Annu. Rev. Immunol.* 22: 817–890.
6. Kawano, T., J. Cui, Y. Koezuka, I. Toura, Y. Kaneko, K. Motoki, H. Ueno, R. Nakagawa, H. Sato, E. Kondo, et al. 1997. CD1d-restricted and TCR-mediated activation of Vα14 NKT cells by glycosylceramides. *Science* 278: 1626–1629.
7. Brossary, L., M. Chioda, N. Burdin, Y. Koezula, G. Casorati, P. Dellabona, and M. Kronenberg. 1998. CD1d-mediated recognition of an α-glycosylceramide by natural killer cells is highly conserved through mammalian evolution. *J. Exp. Med.* 188: 1521–1528.
8. Wilson, S., S. C. Kent, H. F. Horton, A. A. Hill. P. L. Bollyky, D. A. Hafler, J. L. Strominger, and M. C. Byrne. 2000. Multiple differences in gene expression in regulatory Vα24JαQ T cells from identical twins discordant for type I diabetes. *Proc. Natl. Acad. Sci. USA* 97: 7411–7416.
9. Kukreja, A., G. Coat, J. Marker, C. Zhang, Z. Sun, K. Lin-Su, S. Ten, M. Sanz, M. Exley, B. Wilson, et al. 2002. Multiple immuno-regulatory defects in type-I diabetes. *J. Clin. Invest.* 109: 131–140.
10. Sumida, T., A. Sakamoto, H. Murata, Y. Makino, H. Takahashi, S. Yoshida, K. Nishioka, I. Iwamoto, and M. Taniguchi. 1995. Selective reduction of T cells bearing invariant Vα24JαQ antigen receptor in patients with systemic sclerosis. *J. Exp. Med.* 182: 1163–1168.
11. van der Vliet, H. J., B. M. von Blomberg, N. Nishi, M. Rejim, A. E. Voskury, A. A. van Bodegraven, C. H. Polman, T. Rustemeyer, P. Lips, A. J. van den Eertwegh, et al. 2001. Circulating $V\alpha24^+V\beta11^+$ NKT cell numbers are decreased in a wide variety of diseases that are characterized by autoreactive tissue damage. *Clin. Immunol.* 100: 144–148.
12. Kojo, S., Y. Adachi, H. Keino, M. Taniguchi, and T. Sumida. 2001. Dysfunction of T cell receptor $AV24AAJ18^+$, $BV11^+$ double-negative regulatory natural killer T cells in autoimmune diseases. *Arthritis Rheum.* 44: 1127–1138.
13. Illes, Z., T. Kondon, J., Newcombe, N. Oka, T. Tabira, and T. Yamamura. 2000. Differential expression of NKT cell Vα24JαQ invariant TCR chain in the lesions of multiple sclerosis and chronic inflammatory demyelinating polyneuropathy. *J. Immunol.* 164: 4375–4381.
14. Gausling, R., C. Trollmo, and D. A. Hafler. 2001. Decreases in interleukin-4 secretion by invariant $CD4^-CD8^-V\alpha24J\alpha Q$ T cells in peripheral blood of patients with relapsing-remitting multiple sclerosis. *Clin. Immunol.* 98: 11–17.
15. Baxter, A. G., S. J. Kinder, K. J. Hammond, R. Scollay, and D. I. Godfrey. 1997. Association between $\alpha\beta TCR^+CD4^-D8^-$ T-cell deficiency and IDDM in NOD/Lt mice. *Diabetes* 46: 572–582.
16. Frey, A. B., and T. D. Rao. 1999. NKT cell cytokine imbalance in murine diabetes mellitus. *Autoimmunity* 29: 201–214.
17. Yang, Y., M. Bao, and J. W. Yoon. 2001. Intrinsic defects in the T-cell lineage results in natural killer T-cell deficiency and the development of diabetes in the nonobese diabetes mouse. *Diabetes* 50: 2691–2699.
18. Hong, S., M. T. Wilson, I. Serizawa, L. Wu, N. Singh, O. V. Naidenko, T. Miura, T. Haba, D. C. Schere, J. Wei, et al. 2001. The natural killer T-cell ligand α-galactosylceramide prevents autoimmune diabetes in non-obese diabetic mice. *Nat. Med.* 7: 1052–1056.
19. Sharif, S., G. A. Arreaza, P. Zucker, Q. S. Mi, J. Sondhi, O. V. Naidenko, M. Kronenberg, Y. Koezuka, T. L. Delovitch, J. M. Gombert, et al. 2001. Activation of natural killer T cells by α-galactosylceramide treatment prevents the onset and recurrence of autoimmune type I diabetes. *Nat. Med.* 7: 1057–1062.
20. Lehuen, A., O. Lantz, L. Beaudoin, V. Laloux, C. Carnaud, A. Bendelac, J. F. Bach, and R. C. Monteiro. 1998. Overexpression of natural killer T cells protects Vα14-Jα281 transgenic nonobese diabetic mice against diabetes. *J. Exp. Med.* 188: 1831–1839.
21. Wang, B., Y. B. Geng, and C. R. Wang. 2001. CD1-restricted NK T cells protect nonobese diabetic mice from developing diabetes. *J. Exp. Med.* 194: 313–320.
22. Shi, F. D., M. Flodstrom, B. Balasa, S. H. Kim, K. Van Gunst, J. L. Strominger, S. B. Wilson, and N. Sarvetnick. 2001. Germ line deletion of the CD1 locus exacerbates diabetes in the NOD mouse. *Proc. Natl. Acad. Sci. USA* 98: 6777–6782.
23. Mieza, M. A., T. Itoh, J. Q. Cui, Y. Makino, T. Kawano, K. Tsuchida, T. Koike, T. Shirai, H. Yagita, A. Matsuzawa, et al. 1996. Selective reduction of $V\alpha14^+$ NK T cells associated with disease development in autoimmune-prone mice. *J. Immunol.* 156: 4035–4040.
24. Yang, J. Q., V. Saxena, H. Xu, L. Van Kaer, C. R. Wang, and R. R. Singh. 2003. Repeated α-galactosylceramide administration results in expansion of NK T cells and alleviates inflammatory dermatitis in MRL-*lpr/lpr* mice. *J. Immunol.* 171: 4439–4446.
25. Singh, A. K., M. T. Wilson, S. Hong, D. Olivares-Villagómez, C. Du, A. K. Stanic, S. Joyce, S. Sriram, Y. Koezuka, and L. V. Kaer. 2001. Natural killer T cell activation protects mice against experimental autoimmune encephalomyelitis. *J. Exp. Med.* 194: 1801–1811.
26. Miyamoto, K., S. Miyake, and T. Yamamura. 2001. A synthetic glygolipid prevents autoimmune encephalomyelitis by inducing Th2 bias of natural killer T cells. *Nature* 413: 531–534.
27. Chiba, A., S. Oki, K. Miyamato, H. Hashimoto, T. Yamamura, and S. Miyake. 2004. Suppression of collagen-induced arthritis by natural killer T cell activation with OCH, a sphingosine-truncated analog of α-galactosylceramide. *Arthritis Rheum.* 50: 305–313.
28. Ohnishi, Y., A. Tsutsumi, D. Goto, S. Itoh, I. Matsumoto, M. Taniguchi, and T. Sumida. 2005. TCR Vα14 natural killer T cells function as effector T cells in mice with collagen-induced arthritis. *Clin. Exp. Immunol.* 141: 47–53.
29. Zeng, D., M.-K. Lee, J. Tung, A. Brendolan, and S. Stober. 2000. Cutting edge: A role for CD1 in the pathogenesis of lupus in NZB/NZW mice. *J. Immunol.* 164: 5000–5004.
30. Morshed, S. R. M.,. K. Mannoor, R. C. Halder, H. Kawamura, M. Bannai, H. Sekikawa, H. Watanabe, and T. Abo. 2002. Tissue-specific expansion of NKT and $CD5^+$ B cells at the onset of autoimmune disease in $(NZB \times NZW)F_1$ mice. *Eur. J. Immunol.* 32: 2551–2561.
31. Zeng, D., Y. Liu, S. Sidobre, M. Kronenberg, and S. Strober. 2003. Activation of natural killer T cells in NZB/W mice induces Th1-type immune responses exacerbating lupus. *J. Clin. Invest.* 112: 1211–1222.
32. Forestier, C., A. Molano, J. S. Im, Y. Dutronc, B. Diamond, A. Davidson, P. A. Illarionov, G. S. Besra, and S. A. Porcelli. 2005. Expansion and hyperactivity of CD1d-restricted NKT cells during the progression of systemic lupus erythematosus in (New Zealand Black × New Zealand White)F_1 mice. *J. Immunol.* 175: 763–770.
33. Shirai, T., S. Hirose, T. Okada, and H. Nishimura. 1991. Immunology and immunopathology of the autoimmune disease of NZB and related mouse strains. In *Immunological Disorders in Mice*. B. Říhová and V. Vetvicka, eds. CRC Press, Boca Raton, FL, pp. 95–136.
34. Burdin, N., L. Brossay, Y. Koezuka, S. T. Smiley, M. J. Grusby, M. Gui, M. Taniguchi, K, Hayakawa, and M. Kronenberg. 1998. Selective ability of mouse CD1 to present glycolipids: α-galactosylceramide specifically stimulates $V\alpha14^+$ NK T lymphocytes. *J. Immunol.* 161: 3271–3281.
35. Knight, J. G., D. D. Adams, and H. D. Purves. 1977. The genetic contribution of the NZB mouse to the renal disease of the NZB × NZW hybrid. *Clin. Exp. Immunol.* 28: 352–358.
36. Hirose, S., R. Nagawas, I. Sekikawa, M. Hamaoki, Y. Ishida, H. Sato, and T. Shirai. 1983. Enhancing effect of H-2-linked NZW gene(s) on the autoimmune traits of $(NZB \times NZW)F_1$ mice. *J. Exp. Med.* 158: 228–233.
37. Hirose, S., G. Ueda, K. Noguchi, T. Okada, I. Sekikawa, H. Sato, and T. Shirai. 1986. Requirement of H-2 heterozygosity for autoimmunity in $(NZB \times NZW)F_1$ hybrid mice. *Eur. J. Immunol.* 16: 1631–1633.
38. Hirose, S., K. Kinoshita, S. Nozawa, H. Nishimura, and T. Shirai. 1990. Effects of major histocompatibility complex on autoimmune disease of H-2-congenic New Zealand mice. *Int. Immunol.* 2: 1091–1095.
39. Matsuki, N., A. K. Stanic, M. E. Embers, L. V. Kaer, L. Morel, and S. Joyce. 2003. Genetic dissection of Vα14Jα18 natural killer T cell number and function in autoimmune-prone mice. *J. Immunol.* 170: 5429–5437.
40. Kawamura, H., T. Kawamura, Y. Kokai, M. Mori, A. Matsuura, H. Oya, S. Handa, S. Suzuki, A. Weerashinghe, H. Watanabe, and T. Abo. 1999. Expansion of extrathymic T cells as well as granulocytes in the liver and other organs of granulocyte-colony stimulating factor transgenic mice: why they lost the ability of hybrid resistance. *J. Immunol.* 162: 5957–5964.
41. Crough, T., M. Nieda, and A. J. Nicol. 2004. Granulocyte colony-stimulating factor modulates α-galactosylceramide-responsive human $V\alpha24^+V\beta11^+$ NKT cells. *J. Immunol.* 173: 4960–4966.
42. Gorham, J. D., M. L. Güler, R. G. Steen, A. J. Mackey, M. J. Daly, K. Fredrick, W. F. Dietrich, and K. M. Murphy. 1996. Genetic mapping of a murine locus controlling development of T helper 1/T helper 2 type responses. *Proc. Natl. Acad. Sci. USA* 93: 12467–12472.
43. Kuchroo, V. K., D. T. Umetsu, R. H. DeKruyff, and G. J. Freeman. 2003. The TIM gene family: emerging roles in immunity and disease. *Nat. Rev. Immunol.* 3: 454–462.
44. Wills-Karp, M., Y. Belkaid, and C. L. Karp. 2003. I-Tim-izing the pathways of counter-regulation. *Nat. Immunol.* 4: 1050–1052.
45. Shiroiwa, W., K. Tsukamoto, M. Ohtsuji, Q. Lin, A. Ida, S. Kodera, N. Ohtsuji, K. Nakamura, H. Tsurui, K. Kinoshita, et al. 2006. IL-4Rα polymorphism in regulation of IL-4 synthesis by T cells: implication in susceptibility to a subset of murine lupus. *Int. Immunol.* 19: 175–183.
46. Bendelac, A., M. Bonnevillw, and J. F. Kearney. 2001. Autoreactivity by design: innate B and T lymphocytes. *Nat. Rev. Immunol.* 1: 177–186.
47. Zhou, D., J. Mattner, C. Canti, III, N. Schrantz, N. Yin, Y. Gao, Y. Sagiv, K. Hudspeth, Y.-P. Wu, T. Yamashita, et al. 2004. Lysosomal glycosphingolipid recognition by NKT cells. *Science* 306: 1786–1789.
48. Bendelac, A., P. B. Savage, and L. Teyton. 2006. The biology of NKT cells. *Annu. Rev. Immunol.* 25: 297–336.
49. Spolski, R., and W. J. Leonard. 2007. Interleukin-21: basic biology and implications for cancer and autoimmunity. *Annu. Rev. Immunol.* 26: 57–79.
50. Hasegawa, K., M. Abe, T. Okada, S. Hirose, H. Sato, and T. Shirai. 1988. Are Ly1 B cells responsible for the IL2-hyperresponsiveness of B cells in autoimmune-prone NZB × NZW F_1 mice? *Int. Immunol.* 1: 99–103.
51. Taki, S., S. Hirose, K. Kinoshita, H. Nishimura, T. Shimamura, J. Hamuro, and T. Shirai. 1992. Somatically mutated IgG anti-DNA antibody clonally related to germ-line encoded IgM anti-DNA antibody. *Eur. J. Immunol.* 22: 987–992.
52. Hirose, S., M. Wakiya, Y. Kawano-Nishi, Y. Jiang, R. Sanokawa, S. Taki, T. Shimamura, K. Kinoshita, H. Tsurui, H. Nishimura, and T. Shirai. 1993. Somatic diversification and affinity maturation of IgM and IgG anti-DNA antibodies in murine lupus. *Eur. J. Immunol.* 23: 2813–2820.

Available online at www.sciencedirect.com
ScienceDirect
Biochemical and Biophysical Research Communications 367 (2008) 311–317
BBRC
www.elsevier.com/locate/ybbrc

Conservative sequences in 3′UTR of TCRζ mRNA regulate TCRζ in SLE T cells

Kensei Tsuzaka [a,b,*], Yuka Itami [b], Chika Kumazawa [b], Miyuki Suzuki [a], Yumiko Setoyama [a], Keiko Yoshimoto [b], Katsuya Suzuki [a], Tohru Abe [a], Tsutomu Takeuchi [a,b]

[a] *Division of Rheumatology, Department of Internal Medicine, Saitama Medical Center, Saitama Medical University, 1981 Kamoda, Kawagoe, Saitama 350-8550, Japan*

[b] *Project Research Division, Research Center for Genomic Medicine, Saitama Medical University, 1397-1 Yamane, Hidaka, Saitama 350-1241, Japan*

Received 3 December 2007
Available online 3 January 2008

Abstract

We have demonstrated that T-cell receptor ζ (ζ) mRNA with a 562-bp deleted alternatively spliced 3′-untranslated region (3′UTR) observed in T cells of patients with systemic lupus erythematosus (SLE) can lead to a reduction in ζ and TCR/CD3 (J. Immunol., 2003 & 2005). To determine the region in ζ mRNA 3′UTR for the regulation of ζ, ζ mRNA with 3′UTR truncations ligated into pDON-AI was used to infect murine T-cell hybridoma MA5.8 cells, which do not contain ζ. As a Western blot analysis demonstrated the importance of the regions from +871 to +950, containing conservative sequence 1 (CS1), and +1070 to +1136, containing CS2, for the production of ζ, we constructed MA5.8 mutants carrying ζ mRNA 3′UTR with deletions of these regions (ΔCS1 and ΔCS2 mutants). Western blot and FACS analyses showed significant reduction in the cell surface ζ and TCR/CD3 in both these mutants, and IL-2 production was decreased, compared with MA5.8 cells transfected with wild-type ζ mRNA. Furthermore, real-time PCR demonstrated the instability of ζ mRNA with 3′UTR deletions in these MA5.8 mutants. In conclusion, CS1 and CS2 may be responsible for the regulation of ζ and TCR/CD3 through the stability of ζ mRNA in SLE T cells.

Keywords: Systemic lupus erythematosus; TCRζ; 3′UTR; Signal transduction; Conservative sequence; T-cell receptor; IL-2; Autoimmune disease; MA5.8 cells; mRNA stability

Systemic lupus erythematosus (SLE) is well known as a prototype systemic autoimmune disease [1]. Defects in signal transduction through the TCR/CD3 complex may cause T-cell dysfunction and autoimmunity in NOD mice as well as in MRL *lpr/lpr* mice [2–4]. Several studies, including our own, have identified a functional defect in early signaling molecules on peripheral blood T cells (PBTs) as a cause of T-cell dysfunction in human SLE [5–7]. Sakaguchi et al. [8] demonstrated that a ZAP-70 mutation causes autoimmune arthritis in the SKG mouse model, supporting the notion that functional defects in early signaling molecules can cause autoimmune diseases. On the other hand, we and other groups have reported that a reduction in tyrosine phosphorylation and the diminished expression of ζ protein play crucial roles in the pathogenesis of SLE [9–13], and that an aberrant form of the ζ mRNA 3′-untranslated region (3′UTR), which is alternatively spliced and 562-bp shorter than the wild-type 3′UTR, is predominantly expressed in SLE T cells (ζmRNA/as-3′UTR) [14,15] and leads to the up-regulation of several other proteins [16]. An *in vitro* expression analysis of the ζ protein from ζmRNA/as-3′UTR using MA5.8 cell mutants and a retrovirus system showed that the predominant expression of ζmRNA/as-3′UTR leads to the down-regulation of not only ζ, but also of other TCR/CD3 components because of the instability of these ζ mRNA splice variant forms [17]. Observations in our study

* Corresponding author. Fax: +81 49 228 3574.
E-mail address: kentsu@saitama-med.ac.jp (K. Tsuzaka).

0006-291X/$ - see front matter © 2007 Elsevier Inc. All rights reserved.
doi:10.1016/j.bbrc.2007.12.145

[17] and others [18] suggest that the deleted 562-bp portion of the 3′UTR in ζmRNA/as-3′UTR is critical for ζ mRNA stability. The 3′UTR region of mRNA is known to control the turnover rate of pre-synthesized mRNAs through interactions with *trans*-acting factors by altering mRNA stability and affecting the transportation and localization of mRNA [19–21]. Messenger RNA 3′UTR contains *cis*-acting elements, i.e., adenosine-uridine (AU)-rich elements (AREs), that bind to *trans*-acting proteins and participate in either the stabilization or destabilization of transcripts. Two AREs are located at positions +735 and +803 of the ζ mRNA 3′UTR, and both of these AREs are involved in the 562-bp deleted portion of the ζmRNA/as-3′UTR. Therefore, we investigated which portion, including the AREs in the ζ mRNA 3′UTR, could be responsible for the stability of ζ mRNA and the production of the TCR/CD3 complex, including ζ, using MA5.8 cell mutants and a retrovirus system. In this study, we demonstrated that two conservative sequences (CSs), rather than the AREs, are important for the production of the TCR/CD3 complex, including ζ, by influencing ζ mRNA stability.

Materials and methods

RT-PCR. RT-PCR was performed according to a previously described method [13,22]. Human ζ cDNA with 3′UTR truncations (740, 871, 950, 1070, 1136, 1330, and 1457) were amplified from the PBTs of a normal healthy control subject using primers that were designed as described in Table 1 on line. The primers for amplifying the murine CD3ε and β-actin cDNA were arranged as previously reported [22].

Cell lines and inhibition of RNA synthesis. The MA5.8 cells (lacking endogenous ζ expression) were kindly provided by Dr. Takashi Saito and the RetroPack™PT67 (BD Biosciences Clontech, Inc., Palo Alto, CA, USA) was used as the dualtropic packaging cell line. Inhibition of RNA synthesis was performed as previously reported [17].

Construction of MA5.8 mutants. MA5.8 mutants were constructed using a previously described method [17,23]. To construct the MA5.8 mutants with ζmRNA 3′UTR deletions, Fragments A, B, C, and D were amplified from the PBTs of a normal healthy control subject using primers that were designed as described in Table 1 on line. Fragment A and B or Fragment C and D were ligated into SalI-cut pDON-AI and were then transfected into RetroPack™PT67 cells.

Real-time PCR. The primers and TaqMan probes for human ζ, murine CD3 ε, and murine β-actin were designed as previously reported [23]. Amplification and detection of specific products were performed according to a previously described amplification protocol [17]. Standard curves for the quantification of mRNA were established as previously reported [23].

Western blot. Western blot was performed according to a previously described method [9]. The blots were probed with a mouse anti-human ζ mAb (TIA-2) (Coulter Immunology, Hialeah, FL, USA). TIA-2 was visualized using a peroxidase-conjugated anti-mouse IgG (GE Healthcare Bio-Science Corp., Piscataway, NJ, U.S.A.). Biotinylated proteins were detected using streptavidin-peroxidase (Southern Biotechnology Associates, Birmingham, IL, USA). The densities of the specific bands were quantified as index values using the method previously reported [17].

Flow cytometry. The flow cytometric analysis procedure has been previously described [17].

Antibody stimulation and IL-2 quantification. IL-2 quantification was determined by the method described previously [23].

Statistical analysis. Statistical significance was calculated using the Student *t*-test for unpaired data and Statview software (version 4.5; Abacus, Berkeley, CA, USA). A value of $p < 0.05$ was considered statistically significant.

Results

RT-PCR of ζ mRNA with 3′UTR truncations

To identify the region of the ζ mRNA 3′UTR responsible for the expression of ζ and the TCR/CD3 complex, human ζ cDNA with 3′UTR truncations (740 [605 bp], 871 [736 bp], 950 [815 bp], 1070 [935 bp], 1136 [1001 bp], 1330 [1195 bp], and 1457 [1322 bp]) were amplified from the PBTs of a normal healthy control (Fig. 1 on line).

Construction of MA5.8 mutants with ζ mRNA 3′UTR truncations

ζ cDNA with 3′UTR truncations (740, 871, 950, 1070, 1136, 1330, and 1457) were ligated into pDON-AI, transfected into RetroPack™PT67 cells, and used to infect MA5.8 cells to construct the MA5.8 mutants 740, 871, 950, 1070, 1136, 1330, and 1457, respectively. Also, WT and AS3′UTR mutants were constructed from full-length wild-type human ζcDNA and ζcDNA/as-3′UTR, respectively. The NEG mutant was constructed using pDON-AI without any insert DNA.

ζ protein expression in MA5.8 mutants with ζ mRNA 3′UTR truncations

In a Western blot analysis using an anti-human ζ mAb (TIA-2), the production of the ζ protein by the 740 and 871 mutants was not observed (Fig. 1). The production of ζ protein by the 1136 (15.4 index), 1330 (16.7 index), and 1457 (17.2 index) mutants was almost the same as that of the WT mutant (18.5 index). However, the ζ protein expression of the 950 (11.0 index) and 1070 (10.2 index) mutants was relatively low. Therefore, we concluded that ζ protein expression gaps might exist between the 871 and 950 mutants and between the 1070 and 1136 mutants.

Construction of MA5.8 mutants with ζ mRNA 3′UTR deletions

To determine whether the ζ mRNA 3′UTR regions from +871 to +950 and/or from +1070 to +1136 were responsible for the production of ζ protein, we constructed MA5.8 mutants containing ζ mRNA 3′UTR deletions of these two regions. Fragments A (736 bp, +136 to +871), B (680 bp, +952 to +1631), C (940 bp, +136 to +1075), and D (525 bp, +1107 to +1075) were amplified using RT-PCR (Fig. 2 on line). Then, Fragments A and B and Fragments C and D were ligated into pDON-AI, transfected into RetroPack™PT67 cells, and used to infect MA5.8 cells for the construction of the mutants. As the regions from +871 to +950 and +1070 to +1136 contain CS1 (5′-CCCUGCC UUGGGCCCUCUGGUUUGC-3′) and CS2 (5′-C

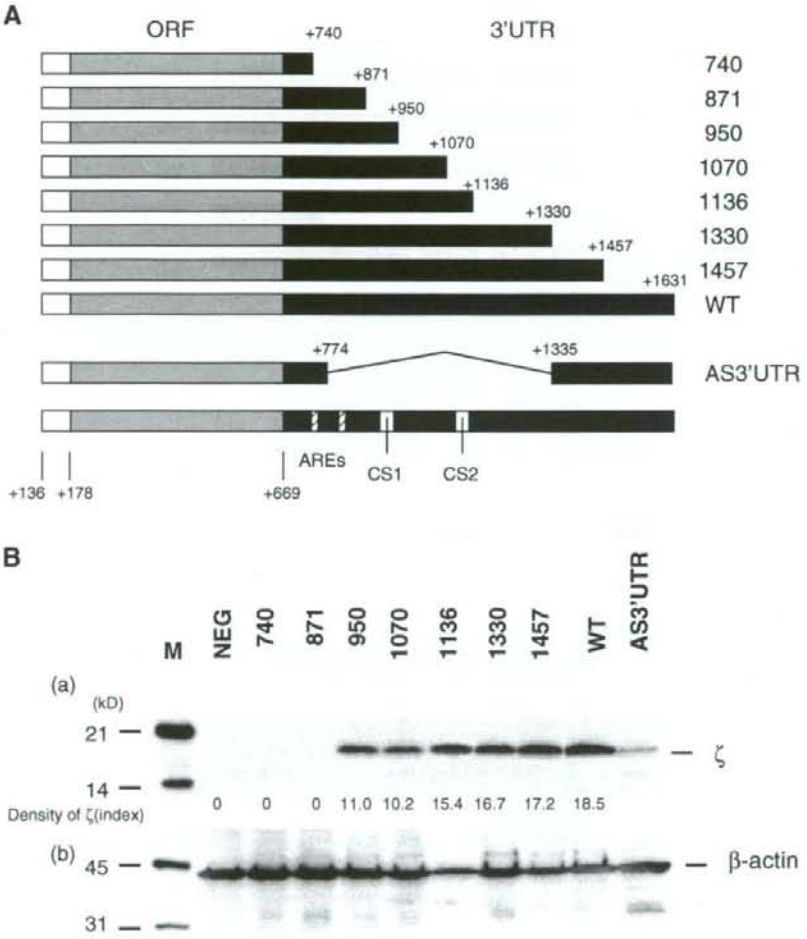

Fig. 1. (A) Scheme of human ζ cDNA with 3′UTR truncations. The shaded bars show the open reading frame (ORF), and the black bars represent the 3′UTR. The white bars show the 5′UTR. AS3′UTR refers to the ζ mRNA/as-3′UTR with a 562-bp deletion (+774 to +1335) in its 3′UTR. The wild-type ζ mRNA 3′UTR contains two A-U rich elements (AREs) (+735 and +803) and two conservative sequences (CSs: CS1, +872 to +951 and CS2, +1076 to +1106). (B) Expression of the ζ protein in MA5.8 mutants with ζ mRNA 3′UTR truncations. Cell lysates from MA5.8 and its mutants (NEG, 740, 871, 950, 1070, 1136, 1330, 1457, WT, and AS3′UTR) were electrophoresed on 15% SDS–polyacrylamide gels using a reducing method and blotted onto a PVDF membrane. The membranes were then incubated with (a) a mouse anti-human ζ mAb (TIA-2) or (b) a hamster anti-mouse β-actin mAb followed by a peroxidase-conjugated anti-mouse IgG. After treatment with chemiluminescence-enhancing reagents, the membranes were visualized on ECL X-ray films, and the densities of the 18-kDa ζ protein bands were quantified as index values.

UCCUGCUGUAAAUUUGGCUUCUGUUGUCAC-3′) (Fig. 3 on line), we defined these MA5.8 mutants as ΔCS1, and ΔCS2 mutants, respectively.

ζ protein expression in MA5.8 mutants with ζ mRNA 3′UTR CS deletions

The expression of the ζ protein in MA5.8 mutants with ζ mRNA 3′UTR CS deletions was analyzed using a Western blot and TIA-2. As shown in Fig. 2, ζ production in both the ΔCS1 and ΔCS2 mutants was slightly higher than that in the AS3′UTR but was significantly lower than that in the WT mutant. From these observations, we concluded that the ζ mRNA 3′UTR regions from +871 to +950 including CS1 and from +1070 to +1136 including CS2 were important for the production of ζ protein.

Expression of ζ and TCR/CD3 complex on the cell surfaces of MA5.8 mutants with ζ mRNA 3′UTR CS deletions

We investigated the expression of ζ and the TCR/CD3 complex on the cell surfaces of these MA5.8 mutants carrying ζ mRNA 3′UTR CS deletions using a FACS analysis. As shown in Fig. 3, the expression of ζ protein on the cell surfaces of both the ΔCS1 (mean channel fluorescence: 73.44) and the ΔCS2 (51.89) was much lower than that of

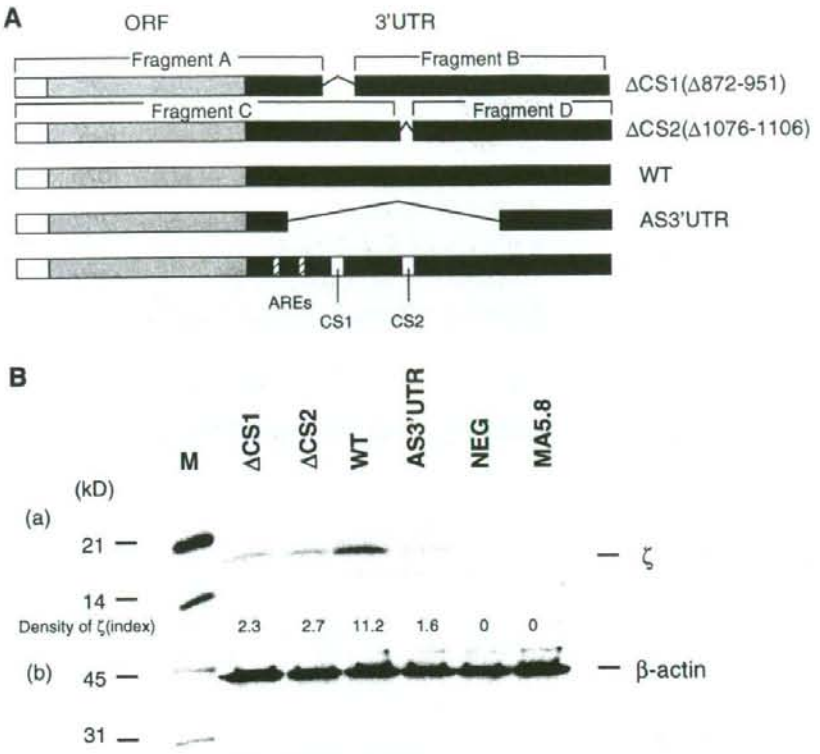

Fig. 2. (A) Scheme of the constructed ζ cDNA with 3′UTR CS deletions. Fragments A and B were ligated into SalI-cut pDON-AI to construct the ζ cDNA with the +872 to +951 deletion (ΔCS1). Fragments C and D were ligated to construct the ζ cDNA with the +1076 to +1106 deletion (ΔCS2). The shaded bars show the ORF, and the black bars represent the 3′UTR. The white bars show the 5′UTR. (B) Expression of the ζ protein in MA5.8 mutants with ζ mRNA 3′UTR CS deletions. Cell lysates from MA5.8 cells and its mutants (ΔCS1, ΔCS2, WT, AS3′UTR, NEG, MA5.8) were electrophoresed on 15% SDS–polyacrylamide gels using a reducing method and blotted onto a PVDF membrane. The membranes were then incubated with (a) a mouse anti-human ζ mAb (TIA-2) or (b) a hamster anti-mouse β-actin mAb followed by a peroxidase-conjugated anti-mouse IgG. After treatment with chemiluminescence-enhancing reagents, the membranes were visualized on ECL X-ray films, and the densities of the 18-kDa ζ protein bands were quantified as index values.

the WT mutant (138.34). Also, the production of TCR/CD3 complex on the cell surfaces of these two MA5.8 mutants with 3′UTR mRNA CS deletions, as estimated by examining CD3 ε expression, was much lower than that of the WT mutants (40.23).

Decrease in IL-2 production in MA5.8 mutants with ζ mRNA 3′UTR CS deletions

To evaluate the physiological effect of the ζ mRNA with 3′UTR CS deletions, MA5.8 mutants were stimulated with anti-mouse CD3 ε mAb (Fig. 4 on line). IL-2 production in the WT mutant on Day 1, 2, or 3 after stimulation was compared statistically with that in the ΔCS1, ΔCS2, or NEG mutant. IL-2 production in the ΔCS1 and ΔCS2 mutants on Day 1 to 3 was significantly ($p < 0.001$) lower than that in the WT mutants on Day 1 to 3, respectively. Consequently, IL-2 production in the MA5.8 mutants with ζ mRNA 3′UTR CS deletions seemed to be lower than usual.

ζ mRNA stability assay

To evaluate the relationship between the reduction in ζ protein expression and the ζ mRNA with 3′UTR CS deletions, we examined the stability of these ζ mRNA. The WT, ΔCS1, and ΔCS2 mutants were cultured and incubated with actinomycin D, and the cells were collected at 0, 6, 12, 24, and 48 h after drug exposure. ζ, CD3 ε, and β-actin cDNA in the WT, ΔCS1, or ΔCS2 mutants were quantified using real-time PCR.

As shown in Fig. 4, the relative amount of ζ mRNA in the ΔCS1 and ΔCS2 mutants rapidly decreased after treatment with actinomycin D and was significantly ($p < 0.01$) lower than that in the WT mutant over time. On the other hand, no significant decrease in the relative amount of CD3 ε mRNA, compared with ζ mRNA, was observed over time after actinomycin D treatment in both the ΔCS1 and ΔCS2 mutants. From these observations, we can conclude that the ζ mRNA with the 3′UTR CS deletions was less stable than the

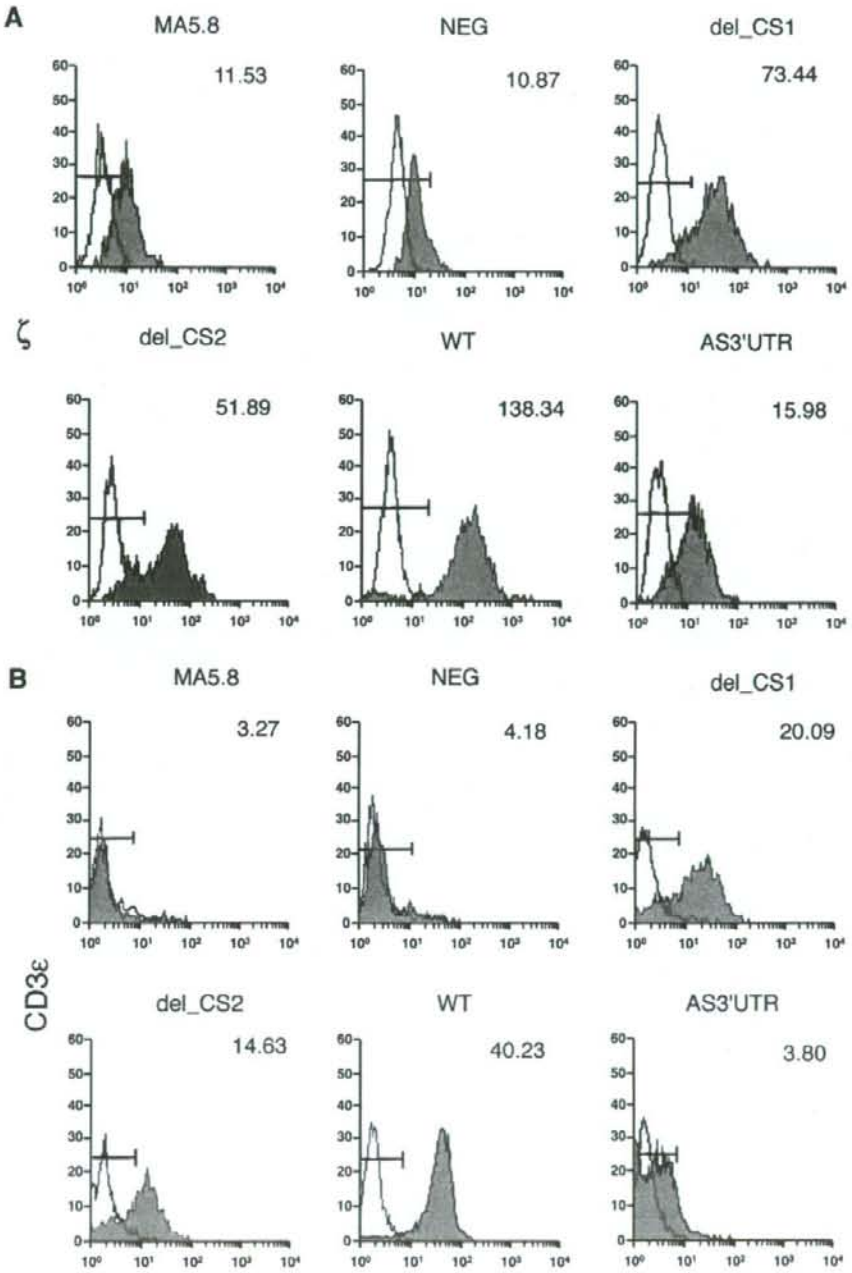

Fig. 3. Flow cytometric analysis of the MA5.8 mutants with ζ mRNA 3′UTR CS deletions. The surface expressions of (A) the ζ protein and (B) the TCR/CD3 complex on MA5.8 cells and its mutants [NEG, del_CS1(ΔCS1), del_CS2(ΔCS2), WT, AS3′UTR] were quantified using FITC-conjugated anti-human ζ mAb (TIA-2) (black profiles) and FITC-conjugated anti-mouse CD3 ε mAb (145-2C11) (black profiles), respectively. An FITC-conjugated mouse anti-human IgG (open profiles in (A)) or FITC-conjugated Armenian hamster anti-mouse IgG (open profiles in (B)) was used as the negative control. The mean channel fluorescence value is indicated within the figures at the *top right*.

wild-type ζ mRNA in the WT mutants. On the other hand, the stability of the CD3 ε mRNA was similar in the MA5.8 mutants with ζ mRNA 3′UTR CS deletions and the WT mutant.

Discussion

In this study, the down-regulation of the ζ protein in the MA5.8 mutants with ζ mRNA 3′UTR CS deletions (ΔCS1,

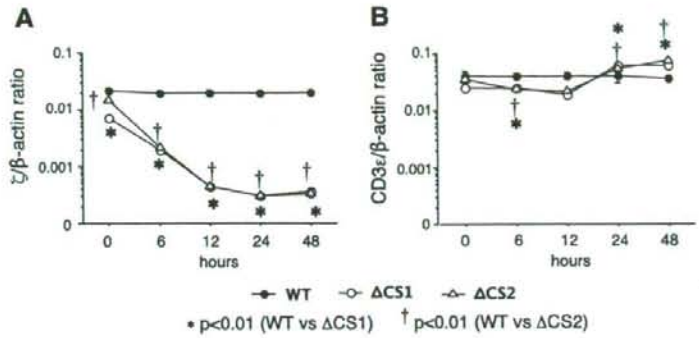

Fig. 4. Decrease in ζ mRNA stability in MA5.8 mutants with ζ mRNA 3′UTR CS deletions. MA5.8 mutants (WT, ΔCS1, ΔCS2) were cultured and incubated with 4 μg/mL of actinomycin D in the culture media. The samples were collected at various time points, and the mRNA was subsequently extracted and converted to whole cDNA. (A) ζ and (B) CD3 ε cDNA were quantified using real-time PCR and were evaluated as the ratio against β-actin cDNA. Each experiment was performed in triplicate. The bars show the mean plus or minus the SD. $^{*}p < 0.01$ for ΔCS1 (open circles) versus WT (closed circles). $^{\dagger}p < 0.01$ for ΔCS2 (open triangles) versus WT (closed circles).

ΔCS2) as confirmed using Western blot and FACS analyses, suggested that the production of the ζ protein was low in the absence of these two CSs of the ζ mRNA 3′UTR. The expression of the TCR/CD3 complex was also decreased in MA5.8 mutants without these regions, as shown by a FACS analysis.

We and other groups have previously reported that the ζ mRNA/as-3′UTR, which is predominantly expressed in SLE T cells, is less stable than the ζ mRNA/w-3′UTR and may be responsible for the reduced expression of the TCR/CD3 complex including ζ protein in SLE T cells [17,18]. Therefore, we examined the stability of ζ mRNA to investigate the reduction in ζ protein expression in the MA5.8 mutants expressing ζ mRNA 3′UTR CS deletions. From our observations, ζ mRNA with 3′UTR CS deletions appeared to be less stable and more easily degraded than ζ mRNA/w-3′UTR. Conceivably, the reduction in the stability of ζ mRNA with 3′UTR CS deletions may lead to a reduction in the expression of the intracellular ζ homodimer, leading to the absence of the expression of the TCR/CD3 complex on the cell surface. Also, the reduction in IL-2 production in these MA5.8 mutants revealed that the signal from the TCR was not transduced into the cytoplasm by anti-CD3 ε antibody stimulation in these mutants. AREs (AUUUA motifs) bind to *trans*-acting proteins and participate in either the stabilization or destabilization of the transcripts. Two AREs, which have been reported to be responsible for the stability of ζ mRNA [24], are located at positions +735 and +803 of ζ mRNA. In our study, however, both MA5.8 mutants 740 and 871 with ζ mRNA 3′UTR truncations did not express ζ protein and MA5.8 mutants ΔCS1 and ΔCS2, which contained the AREs, were easily degraded. From these observations, there might remain the possibility that the AREs at +735 and +803 are not related to the production of ζ protein or the stability of ζ mRNA. However, this possibility can be demonstrated only by using a deletion mutant lacking AREs but containing CSs. This study is now under way in our laboratory. In conclusion, the present study suggests that the regions between +872 and +951 and between +1076 and +1106 in the ζ mRNA 3′UTR are critical for ζ mRNA stability. Gramolini et al. reported that a 171-bp region in the 3′UTR of utrophin mRNA regulates utrophin mRNA stability, since the half-life of utrophin mRNA without this region is much shorter than that of the wild-type mRNA [25]. Also, Akgül et al. reported a 59-nucleotide (nt) pentobarbital-responsive element in the 3′UTR of *Drosophila* glutathione-*S*-transferase D21 (gstD21) mRNA that regulates the stability of gstD21 mRNA [26].

Interestingly, CS1 and CS2 are conserved in several mammals (Fig. 3 on line). Xie et al. reported that 106 CSs in mRNA 3′UTR are involved in post-transcriptional regulation and that half of these CSs are related to AREs, while the other half of the CSs that do not contain AREs are associated with microRNAs [27]. Since both the CS1 and CS2 in the ζ mRNA 3′UTR do not include AREs (AUUUA motifs), some miRNAs might influence the stability of the ζ mRNA by binding to the CS1 and CS2 in ζmRNA 3′UTR regions that do not contain AREs. This possibility is now being studied in our laboratory.

Acknowledgment

This work was supported by Grants-in-Aid for Scientific Research (C) from the Ministry of Education, Science and Culture, Japan.

Appendix A. Supplementary data

Supplementary data associated with this article can be found, in the online version, at doi:10.1016/j.bbrc.2007.12.145.

References

[1] J.A. Mills, Systemic lupus erythematosus, N. Engl. J. Med. 30 (1994) 1871–1879.

[2] D. Zipris, A.H. Lazarus, A.R. Crow, M. Hadzija, T.L. Delovitch, Defective thymic T cell activation by concanavalin A and anti-CD3 in autoimmune nonobese diabetic mice. Evidence for thymic T cell anergy that correlates with the onset of insulitis, J. Immunol. 146 (1991) 3763–3771.

[3] M.A. Berman, C.I. Sandborg, Z. Wang, K.L. Imfeld, F. Zaldivar Jr., V. Dadufalza, B.A. Buckingham, Decreased IL-4 production in new onset type I insulin-dependent diabetes mellitus, J. Immunol. 157 (1996) 4690–4696.

[4] S.B. Wilson, S.C. Kent, K.T. Patton, T. Orban, R.A. Jackson, M. Exley, S. Porcelli, D.A. Schatz, M.A. Atkinson, S.P. Balk, J.L. Strominger, D.A. Hafler, Extreme Th1 bias of invariant Valpha24JalphaQ T cells in type 1 diabetes, Nature 39 (1998) 177–181.

[5] A.K. Dayal, G.M. Kammer, The T cell enigma in lupus, Arthritis Rheum. 39 (1996) 23–33.

[6] S. Sierakowski, E.J. Kucharz, R.W. Lightfoot, J.S. Goodwin, Impaired T-cell activation in patients with systemic lupus erythematosus, J. Clin. Immunol. 9 (1989) 469–476.

[7] T. Takeuchi, M. Pang, K. Amano, J. Koide, T. Abe, Reduced protein tyrosine phosphatase (PTPase) activity of CD45 on peripheral blood lymphocytes in patients with systemic lupus erythematosus (SLE), Clin. Exp. Immunol. 109 (1997) 20–26.

[8] N. Sakaguchi, T. Takahashi, H. Hata, T. Nomura, T. Tagami, S. Yamazaki, T. Sakihama, T. Matsutani, I. Negishi, S. Nakatsuru, S. Sakaguchi, Altered thymic T-cell selection due to a mutation of the ZAP-70 gene causes autoimmune arthritis in mice, Nature 426 (2003) 454–460.

[9] T. Takeuchi, K. Tsuzaka, M. Pang, K. Amano, J. Koide, T. Abe, TCRζ chain lacking exon 7 in two patients with systemic lupus erythematosus, Int. Immunol. 10 (1998) 911–921.

[10] S.N. Liossis, X.Z. Ding, G.J. Dennis, G.C. Tsokos, Altered pattern of TCR/CD3-mediated protein-tyrosyl phosphorylation in T cells from patients with systemic lupus erythematosus. Deficient expression of the T cell receptor ζ chain, J. Clin. Invest. 101 (1998) 1448–1457.

[11] V. Brundula, L.J. Rivas, A.M. Blasini, M. Paris, S. Salazar, I.L. Stekman, M.A. Rodriguez, Diminished levels of T cell receptor ζ chains in peripheral blood T lymphocytes from patients with systemic lupus erythematosus, Arthritis Rheum. 42 (1999) 1908–1916.

[12] M. Pang, Y. Setoyama, K. Tsuzaka, K. Yoshimoto, K. Amano, T. Abe, T. Takeuchi, Defective expression and tyrosine phosphorylation of the T cell receptor ζ chain in peripheral blood T cells from systemic lupus erythematosus patients, Clin. Exp. Immunol. 129 (2002) 160–168.

[13] K. Tsuzaka, T. Takeuchi, N. Onoda, M. Pang, T. Abe, Mutations in T cell receptor ζ chain mRNA of peripheral T cells from systemic lupus erythematosus, J. Autoimmun. 11 (1998) 381–385.

[14] K. Tsuzaka, N. Onoda, K. Yoshimoto, Y. Setoyama, K. Suzuki, M. Pang, T. Abe, T. Takeuchi, T-cell receptor ζ mRNA with alternatively spliced 3′ untranslated region is generated predominantly in the peripheral blood T cells of systemic lupus erythematosus patients, Mod. Rheumatol. 12 (2002) 167–173.

[15] M.P. Nambiar, E.J. Enyedy, V.G. Warke, S. Krishnan, G. Dennis, M. Kammer, G.C. Tsokos, Polymorphisms/mutations of TCR ζ chain promoter and 3′ untranslated region and selective expression of TCR ζ chain with an alternatively spliced 3′ untranslated region in patients with systemic lupus erythematosus, J. Autoimmun. 16 (2001) 133–142.

[16] K. Tsuzaka, K. Nozaki, C. Kumazawa, K. Shiraishi, Y. Setoyama, K. Yoshimoto, K. Suzuki, T. Abe, T. Takeuchi, DNA microarray gene expression profile of T cells with the splice variants of TCRζ mRNA observed in SLE, J. Immunol. 176 (2006) 949–956.

[17] K. Tsuzaka, I. Fukuhara, Y. Setoyama, K. Yoshimoto, K. Suzuki, T. Abe, T. Takeuchi, TCRζ mRNA with an alternatively spliced 3′ untranslated region detected in SLE patients leads to the downregulation of TCRζ and TCR/CD3 complex, J. Immunol. 171 (2003) 2496–2503.

[18] B. Chowdhury, C.G. Tsokos, S. Krishnan, J. Robertson, C.U. Fisher, R.G. Warke, V.G. Warke, M.P. Nambiar, G.C. Tsokos, Decreased stability and translation of T cell receptor ζ mRNA with an alternatively spliced 3′-untranslated region contribute to ζ chain down-regulation in patients with systemic lupus erythematosus, J. Biol. Chem. 280 (2005) 18959–18966.

[19] G. Bassell, R.H. Singer, mRNA and cytoskeletal filaments, Curr. Opin. Cell Biol. 9 (1997) 109–115.

[20] K.C. Tsai, V.V. Cansino, D.T. Kohn, R.L. Neve, N.I. Perrone-Bizzozero, Post-transcriptional regulation of the GAP-43 gene by specific sequences in the 3′ untranslated region of the mRNA, J. Neurosci. 17 (1997) 1950–1958.

[21] J.L. Veyrune, J. Hesketh, J.M. Blanchard, 3′ Untranslated regions of c-myc and c-fos mRNAs: multifunctional elements regulating mRNA translation, degradation and subcellular localization, Prog. Mol. Subcell. Biol. 18 (1997) 35–63.

[22] J.P. Jensen, D. Hou, M. Ramsburg, A. Taylor, M. Dean, A.M. Weissman, Organization of the human T cell receptor ζ/η gene and its genetic linkage to the FcγRII-FcγRIII gene cluster, J. Immunol. 148 (1992) 2563–2571.

[23] K. Tsuzaka, Y. Setoyama, K. Yoshimoto, K. Shiraishi, K. Suzuki, T. Abe, T. Takeuchi, A splice variant of the TCR ζ mRNA lacking exon 7 leads to the down-regulation of TCR ζ, the TCR/CD3 complex, and IL-2 production in SLE T cells, J. Immunol. 174 (2005) 3518–3525.

[24] B. Chowdhury, S. Krishnan, C.G. Tsokos, J.W. Robertson, C.U. Fisher, M.P. Nambiar, G.C. Tsokos, Stability and translation of TCR ζ mRNA are regulated by the adenosine-uridine-rich elements in splice-deleted 3′ untranslated region of ζ -chain, J. Immunol. 177 (2006) 8248–8257.

[25] A.O. Gramolini, G. Belanger, B.J. Jasmin, Distinct regions in the 3′ untranslated region are responsible for targeting and stabilizing utrophin transcripts in skeletal muscle cells, J. Cell Biol. 154 (2001) 1173–1183.

[26] B. Akgül, C-PD. Tu, Regulation of mRNA stability through a pentobarbital-responsive element, Arch. Biochem. Biophys. 459 (2006) 143–150.

[27] X. Xie, J. Lu, E.J. Kulbokas, T.R. Golub, V. Mootha, K. Lindblad-Toh, E.S. Lander, M. Kellis, Systematic discovery of regulatory motifs in human promoters and 3′UTRs by comparison of several mammals, Nature 434 (2005) 338–345.

Mod Rheumatol
DOI 10.1007/s10165-008-0139-8

ORIGINAL ARTICLE

Clinical and histopathological features of myopathies in Japanese patients with anti-SRP autoantibodies

Tetsuya Takada · Michito Hirakata · Akira Suwa · Yuko Kaneko · Masataka Kuwana · Tadayuki Ishihara · Yasuo Ikeda

Received: 13 September 2008 / Accepted: 15 October 2008

Abstract To elucidate the clinical and histopathological features associated with autoantibodies to the signal recognition particle (SRP), we have studied 23 Japanese patients with this specificity among 3,500 patients with polymyositis/dermatomyositis and other connective tissue diseases. Anti-SRP antibodies were determined based on analysis of RNA and protein components by immunoprecipitation assays. The pathological analysis was performed by using special stainings including alkaline phosphatase, myosin ATPase, and modified Gomori trichrome stainings. Twenty-one (92%) of these 23 patients had myositis, 8 of whom (38%) required cytotoxic agents or intravenous immunoglobulin therapy in addition to corticosteroid therapy. Four patients (16%) had rheumatoid arthritis, two of whom had no features of myositis. Muscle biopsy specimens of 11 patients were examined histologically in detail. All 11 had muscle fiber necrosis and/or regeneration, but only one had infiltration of inflammatory cells. Six of the 11 (55%) patients showed type I fiber predominance by ATPase staining, while eight control myositis patients without anti-SRP antibodies did not. There was no correlation of other neurogenic features in histology with the presence of anti-SRP antibodies. These studies suggest that anti-SRP autoantibodies are most likely to be related to myopathies that are resistant to corticosteroid therapy and without inflammation histopathologically.

Keywords Anti-SRP antibodies · Histopathology · Muscle biopsy · Myositis-specific autoantibodies · Polymyositis · Dermatomyositis

T. Takada · M. Hirakata (✉) · Y. Kaneko · M. Kuwana · Y. Ikeda
Division of Rheumatology, Department of Internal Medicine, Keio University School of Medicine, 35 Shinanomachi, Shinjuku-ku, Tokyo 160-8582, Japan
e-mail: mhirakat@sc.itc.keio.ac.jp

A. Suwa
Division of Rheumatology, Department of Internal Medicine, Tokai University School of Medicine, Isehara, Kanagawa 259-1193, Japan

T. Ishihara
Hakone National Hospital, Kazamatsuri 412, Odawara, Kanagawa 250-0032, Japan

Introduction

The inflammatory muscle diseases, polymyositis (PM) and dermatomyositis (DM) are systemic connective tissue disorders characterized by chronic inflammation in skeletal muscle and involvement of various internal organs [1]. The pathogenesis of PM/DM is unknown, but appears to result from an autoimmune mechanism that culminates in the tissue damage [2]. Autoantibodies directed against various cellular constituents have been identified in patients with PM/DM, and some of them that are found almost exclusively in PM/DM are known as myositis-specific autoantibodies (MSA) [3–5]. Each MSA is associated with a set of unique clinical features; therefore detection of MSA provides us clinically useful information that helps in diagnosis, patient classification as well as in predicting symptoms, response to treatment, and prognosis [6–9]. Autoantibodies to the cytoplasmic antigens that are involved in protein synthesis or translation are frequently seen in patients with PM [2]. Especially, autoantibodies to eight of the aminoacyl tRNA synthetases (ARS), such as Jo-1 (histidyl tRNA synthetase), are the most common and closely associated with a unique clinical subset called "anti-synthetase syndrome" characterized by myositis,

Published online: 17 December 2008